LBNL-49074
Preprint

ERNEST ORLANDO LAWRENCE BERKELEY NATIONAL LABORATORY

Rare Charm Decays in the Standard Model and Beyond

Gustavo Burdman, Eugene Golowich,
JoAnne Hewett, and Sandip Pakvasa

Physics Division

November 2001

Submitted to
Physical Review D

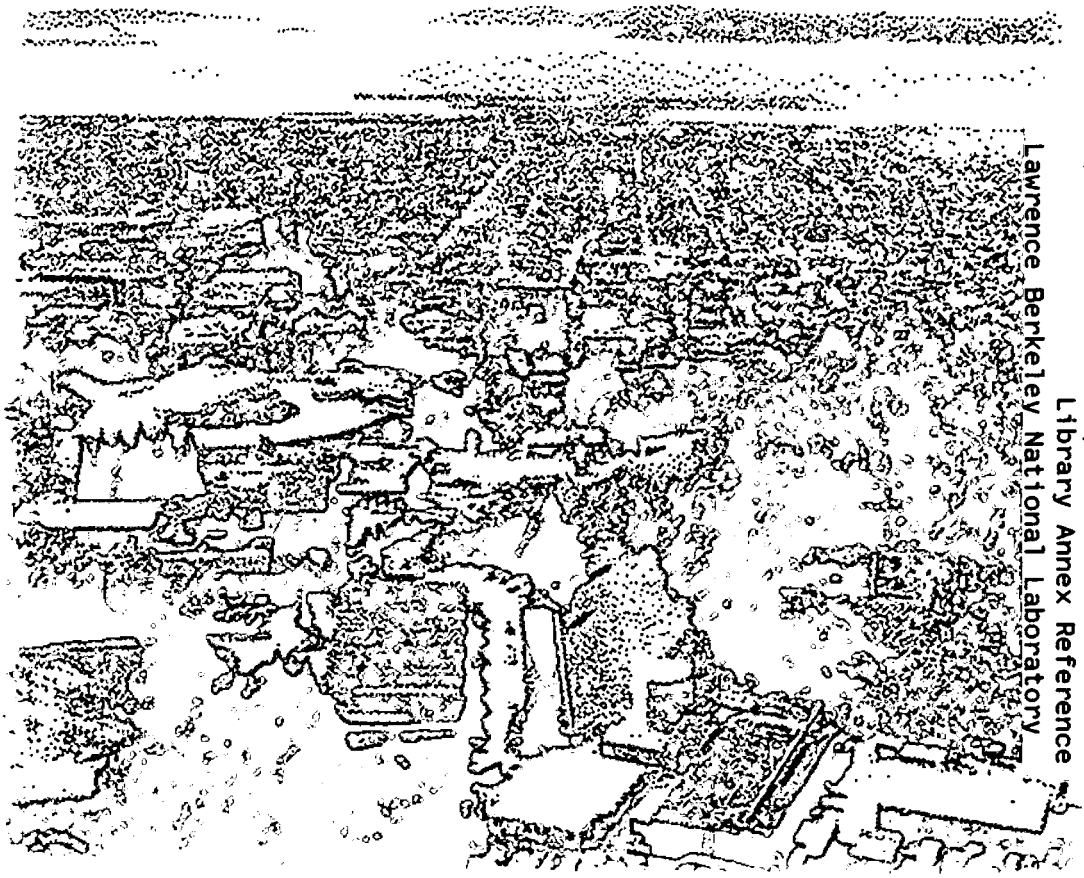

REFERENCE COPY
Does Not
Circulate

Library Annex Reference
Lawrence Berkeley National Laboratory

Copy 1

LBNL-49074

DISCLAIMER

This document was prepared as an account of work sponsored by the United States Government. While this document is believed to contain correct information, neither the United States Government nor any agency thereof, nor the Regents of the University of California, nor any of their employees, makes any warranty, express or implied, or assumes any legal responsibility for the accuracy, completeness, or usefulness of any information, apparatus, product, or process disclosed, or represents that its use would not infringe privately owned rights. Reference herein to any specific commercial product, process, or service by its trade name, trademark, manufacturer, or otherwise, does not necessarily constitute or imply its endorsement, recommendation, or favoring by the United States Government or any agency thereof, or the Regents of the University of California. The views and opinions of authors expressed herein do not necessarily state or reflect those of the United States Government or any agency thereof or the Regents of the University of California.

LBNL-49074

Rare Charm Decays in the Standard Model and Beyond

Gustavo Burdman,[a] Eugene Golowich,[b] JoAnne Hewett,[c] and Sandip Pakvasa[d]

[a]Physics Division
Ernest Orlando Lawrence Berkeley National Laboratory
University of California
Berkeley, CA 94720

[b]Physics Department
University of Massachusetts
Amherst, MA 01003

[c]Stanford Linear Accelerator Center
Stanford, CA 94309

[d]Department of Physics and Astronomy
University of Hawaii
Honolulu, HI 96822

November 2001

This work was supported by the Director, Office of Science, Office of High Energy and Nuclear Physics, and Contract No. DE-FG-03-94ER40833, of the U.S. Department of Energy under Contract No. DE-AC03-76SF00098, and National Science Foundation Grant No. PHY-9801875.

November 14, 2001
LBNL-49074

Rare Charm Decays in the Standard Model and Beyond

Gustavo Burdman[a], Eugene Golowich[b], JoAnne Hewett[c] and Sandip Pakvasa[d]

[a]*Lawrence Berkeley National Laboratory*
Berkeley, CA 94720

[b]*Physics Department, University of Massachusetts,*
Amherst, MA 01003

[c]*Stanford Linear Accelerator Center, Stanford, CA 94309*

[d]*Department of Physics and Astronomy, University of Hawaii,*
Honolulu, HI 96822

Abstract

We consider SM predictions for a number of rare charm decays, distinguishing between short-distance and long-distance contributions. For processes mediated by the $c \to u\ell^+\ell^-$ transitions we show that sensitivity to short distance physics exists in kinematic regions away from the vector meson resonances that dominate the total rate. In particular, we find that $D \to \pi\ell^+\ell^-$ and especially $D \to \rho\ell^+\ell^-$ are sensitive to non-universal soft-breaking effects in the Minimal Supersymmetric Standard Model with R-parity conservation. We separately study the sensitivity of these modes to R-parity violating effects and derive new bounds on R-parity violating couplings. We also obtain predictions for other extensions of the Standard Model, including extensions of the Higgs, gauge and fermion sectors, as well as models of dynamical electroweak symmetry breaking.

1 Introduction

The remarkable success of the Standard Model (SM) in describing all experimental information currently available suggests that the quest for deviations from it should be directed either at higher energy scales or at small effects in low energy observables. To the last group belong the sub-percent level precision measurements of electroweak observables at LEPI and SLD as well as the Tevatron experiments [1]. Tests of the SM through quantum corrections have proven to be a powerful tool to reach the high energy scales possibly related to electroweak symmetry breaking and the flavor problem. The absence of flavor changing neutral currents (FCNC) at tree level in the SM implies that processes involving these currents are a primary test of the quantum structure of the theory. Most of the attention on FCNC has been focused on processes involving K and B mesons, such as $K^0 - \bar{K}^0$ and $B_d^0 - \bar{B}_d^0$ mixings and also on rare decays involving transitions such as $s \to d\ell^+\ell-$, $s \to d\nu\bar{\nu}$, $b \to s\gamma$, $b \to s\ell^+\ell^-$, *etc.*

The analogous FCNC processes in the charm sector have received considerably less scrutiny. This is perhaps due to the fact that, on general grounds, the SM expectations are very small both for $D^0 - \bar{D}^0$ mixing [2,3] as well as for FCNC decays [4,5]. For instance, there are no large non-decoupling effects arising from a heavy fermion in the leading one-loop contributions. This is in sharp contrast with K and B FCNC processes, which are affected by the presence of the top quark in loops. In the SM, D meson FCNC transitions involve the rather light down-quark sector which translates into an efficient GIM cancellation. In many cases, extensions of the SM may upset this suppression and give contributions sometimes orders of magnitude larger than the SM. In this paper we wish to investigate this possibility. As a first step, and in order to establish the existence of a clean window of observation for new physics in a given observable in rare charm processes, we must compute the SM contribution to such quantities. This is of particular importance in this case due to presence of potentially large long-distance contributions which are non-perturbative in essence and therefore non-calculable by analytical methods. In general the flavor structure of charm FCNC favors the propagation of light-quark-states as intermediate states which, if dominant, obscure the more interesting short distance contributions that are the true test of the SM. This is the situation in $D^0 - \bar{D}^0$ mixing [2,3] and in the $c \to u\gamma$ transition [4]. In the case of mixing, although the long distance effects seem to dominate over the SM short distance contributions, it is still possible that there is a window of one or two orders of magnitude between these and the current experimental limit [6]. On the other hand, charm radiative decays are completely dominated by non-perturbative physics and do not constitute a suitable test of the short distance structure of the SM or its extensions.

In what follows we investigate the potential of rare charm decays to constrain extensions of the SM. With the exception of $D^0 \to \gamma\gamma$, we shall concentrate on the non-radiative

FCNC transitions such as $c \to u\ell^+\ell^-$, $c \to u\nu\bar{\nu}$ entering in decays like $D^0 \to \mu^+\mu^-$, $D \to X_u\ell^+\ell^-$, $D \to X_u\nu\bar{\nu}$, *etc.* We extensively consider supersymmetry by studying the Minimal Supersymmetric SM (MSSM) as well as supersymmetric scenarios allowing R-parity violation. We find that rare charm decays are potentially good tests of the MSSM and also serve to constrain R-parity violation couplings in kinematic regions away from resonances. In charged dilepton modes, this mostly means at *low* dilepton mass. In general, we find that this kinematic region, corresponding to large hadronic recoil, is the best for new physics searches.

The $D \to V\ell^+\ell^-$ decays were studied in Ref. [7] in the SM. More recently the $D \to \pi\ell^+\ell^-$ decays were studied in Ref. [8] in the SM and some of its extensions, including the MSSM. We compare these predictions with ours. We find some discrepancies in the SM calculation of the long distance contributions. We also emphasize the importance of $D \to V\ell^+\ell^-$ in the MSSM due to its enhanced sensitivity to the electromagnetic dipole moment operator entering in $c \to u\gamma$.

In the next section we calculate SM short distance contributions and estimate long distance effects for various decay modes. In Section 3 we study possible extensions of the SM that might produce signals which fall below current experimental limits but above SM results of Section 2. We summarize and conclude in Section 4.

As a final comment, we note the following convention and notation used throughout the paper. Many quantities relating to both SM and also NP are chiral, involving projection operators for left-handed (LH) and right-handed (RH) massless fermions. We shall employ the notation

$$\Gamma_{\rm L,R} \equiv \frac{1 \pm \gamma_5}{2}\,, \qquad \Gamma^\mu_{\rm L,R} \equiv \frac{\gamma^\mu(1 \pm \gamma_5)}{2} \tag{1}$$

for scalar projection operators $\Gamma_{\rm L,R}$ and vector projection operators $\Gamma^\mu_{\rm L,R}$. The chiral projections of fermion field q are thus expressed as

$$q_{\rm L,R} \equiv \Gamma_{\rm L,R}\, q \ . \tag{2}$$

2 The Standard Model Contributions

In this section we study Standard Model contributions to various charm meson rare decays. At the time of this writing, there are almost no reported events of the type we are considering. We group the decay modes by their common short distance structure. In each case we address both the perturbative short distance amplitude and the effects of the non-perturbative long-range propagation of intermediate hadronic states. Due to non-perturbative nature of the underlying physics, the long distance effects cannot be calculated with controlled uncertainties. Therefore we find it prudent to generate estimates by using several distinct approaches, such as vector meson dominance (VMD)

for processes with photon emission and/or calculable unitarity contributions. In this way, we hope to obtain a reasonable measure of the uncertainty involved in the calculation, and at the same time, obtain bounds on the importance of long-distance physics which are not overly model dependent.

2.1 Meson Lepton-antilepton Transitions $D \to X\ell^+\ell^-$

As we shall discuss, this mode is likely to be observed at forthcoming experiments to be performed in B and Charm factory/accelerator experiments. We start with the calculation of both short and long distance contributions to the inclusive rate. We then compute the rates for various exclusive modes.

2.1.1 The Short Distance Contribution to $D \to X_u\ell^+\ell^-$

The short distance contribution is induced at one loop in the SM. It is convenient to use an effective description with the W boson integrated out,

$$\mathcal{H}_{\text{eff}} = -\frac{4G_F}{\sqrt{2}} \sum_{i=1}^{10} C_i(\mu) O_i(\mu) \quad , \tag{3}$$

with $\{O_i\}$ being the complete operator basis, $\{C_i\}$ the corresponding Wilson coefficients and μ the renormalization scale. In Eq. (3) the Wilson coefficients contain the dependence on the Cabibbo-Kobayashi-Maskawa (CKM) matrix elements. As was pointed out in Ref. [4], the CKM structure of these transitions is drastically different from that of the analogous B meson processes. The operators O_1 and O_2 are explicitly split into their CKM components

$$O_1^{(q)} = (\bar{u}_L^\alpha \gamma_\mu q_L^\beta)(\bar{q}_L^\beta \gamma^\mu c_L^\alpha) \ , \qquad O_2^{(q)} = (\bar{u}_L^\alpha \gamma_\mu q_L^\alpha)(\bar{q}_L^\beta \gamma^\mu c_L^\beta) \ , \tag{4}$$

where $q = d, s, b$, and α, β are contracted color indices. The rest of the operator basis is defined in the standard way. The QCD penguin operators are given by

$$\begin{aligned} O_3 &= (\bar{u}_L^\alpha \gamma_\mu c_L^\alpha) \sum_q (\bar{q}_L^\beta \gamma^\mu q_L^\beta) \ , \qquad O_4 = (\bar{u}_L^\alpha \gamma_\mu c_L^\beta) \sum_q (\bar{q}_L^\beta \gamma^\mu q_L^\alpha) \ , \\ O_5 &= (\bar{u}_L^\alpha \gamma_\mu c_L^\alpha) \sum_q (\bar{q}_R^\beta \gamma^\mu q_R^\beta) \ , \qquad O_6 = (\bar{u}_L^\alpha \gamma_\mu c_L^\beta) \sum_q (\bar{q}_R^\beta \gamma^\mu q_R^\alpha) \ , \end{aligned} \tag{5}$$

the electromagnetic and chromomagnetic dipole operators are

$$O_7 = \frac{e}{16\pi^2} m_c (\bar{u}_L \sigma_{\mu\nu} c_R) F^{\mu\nu} \ , \qquad O_8 = \frac{g_s}{16\pi^2} m_c (\bar{u}_L \sigma_{\mu\nu} T^a c_R) G_a^{\mu\nu} \ , \tag{6}$$

and finally the four-fermion operators coupling directly to the charged leptons are

$$O_9 = \frac{e^2}{16\pi^2} (\bar{u}_L \gamma_\mu c_L)(\bar{\ell} \gamma^\mu \ell) \ , \qquad O_{10} = \frac{e^2}{16\pi^2} (\bar{u}_L \gamma_\mu c_L)(\bar{\ell} \gamma^\mu \gamma_5 \ell) \ . \tag{7}$$

The matching conditions at $\mu = M_W$ for the Wilson coefficients of the operators O_{1-6} are

$$C_1^q(M_W) = 0 \ , \qquad C_{3-6}(M_W) = 0 \ , \qquad C_2^q(M_W) = -\lambda_q \ , \tag{8}$$

with $\lambda_q = V_{cq}^* V_{uq}$. The corresponding conditions for the coefficients of the operators O_{7-10} are

$$C_7(M_W) = -\frac{1}{2}\left\{\lambda_s F_2(x_s) + \lambda_b F_2(x_b)\right\} \ , \tag{9}$$

$$C_8(M_W) = -\frac{1}{2}\left\{\lambda_s D(x_s) + \lambda_b D(x_b)\right\} \ , \tag{10}$$

$$C_9(M_W) = \sum_{i=s,b} \lambda_i \left[-\left(F_1(x_i) + 2\bar{C}(x_i)\right) + \frac{\bar{C}(x_i)}{2s_w^2} \right] \ , \tag{11}$$

$$C_{10}(M_W) = -\sum_{i=s,b} \lambda_i \frac{\bar{C}(x_i)}{2s_w^2} \ . \tag{12}$$

In Eqs. (9)-(12) we define $x_i = m_i^2/M_W^2$, the functions $F_1(x)$, $F_2(x)$ and $\bar{C}(x)$ are those defined in Ref. [9] and the function $D(x)$ was defined in Ref. [4].

To compute the $c \to u\ell^+\ell^-$ rate at leading order, operators in addition to O_7, O_9 and O_{10} must contribute. Even in the absence of the strong interactions, the insertion of the operators $O_2^{(q)}$ in a loop would give a contribution sometimes referred to as leading order mixing of C_2 with C_9. When the strong interactions are considered, further mixing of the four-quark operators with O_{7-10} occurs. The effect of these QCD corrections in the renormalization group (RG) running from M_W down to $\mu = m_c$ is of particular importance in $C_7^{\rm eff}(m_c)$, the coefficient determining the $c \to u\gamma$ amplitude. As was shown in Ref. [4], the QCD-induced mixing with $O_2^{(q)}$ dominates $C_7^{\rm eff}(m_c)$. The fact that the main contribution to the $c \to u\gamma$ amplitude comes from the insertion of four-quark operators inducing light-quark loops signals the presence of large long distance effects. This was confirmed in Ref. [4] where these non-perturbative contributions were estimated and found to dominate the rate. Therefore, in the present calculation we will take into account effects of the strong interactions in $C_7^{\rm eff}(m_c)$. On the other hand (and as we mentioned above) the operator O_9 mixes with four-quark operators even in the absence of QCD corrections. Finally, the RG running does not affect O_{10}, *i.e.* $C_{10}(m_c) = C_{10}(M_W)$. Thus, in order to estimate the $c \to u\gamma$ amplitude it is a good approximation to consider the QCD effects only where they are dominant, *i.e.* in $C_7^{\rm eff}(m_c)$, whereas we expect these to be less dramatic in $C_9^{\rm eff}(m_c)$.

The leading order mixing of $O_2^{(q)}$ with O_9 results in

$$C_9^{\rm eff} = C_9(M_W) + \sum_{i=d,s,b} \lambda_i \left[-\frac{2}{9}\ln\frac{m_i^2}{M_W^2} + \frac{8}{9}\frac{z_i^2}{\hat{s}} - \frac{1}{9}\left(2 + \frac{4z_i^2}{\hat{s}}\right)\sqrt{\left|1 - \frac{4z_i^2}{\hat{s}}\right|}\,\mathcal{T}(z_i) \right] \ , \tag{13}$$

where we have defined

$$\mathcal{T}(z) = \begin{cases} 2 \arctan\left[\frac{1}{\sqrt{\frac{4z^2}{\hat{s}}-1}}\right] & (\text{for } \hat{s} < 4z^2) \\ \ln\left|\frac{1+\sqrt{1-\frac{4z^2}{\hat{s}}}}{1-\sqrt{1-\frac{4z^2}{\hat{s}}}}\right| - i\pi & (\text{for } \hat{s} > 4z^2) \end{cases} , \tag{14}$$

and $\hat{s} \equiv s/m_c^2$, $z_i \equiv m_i/m_c$. The logarithmic dependence on the internal quark mass m_i in the second term of Eq. (13) cancels against a similar term in the Inami-Lim function $F_1(x_i)$ entering in $C_9(M_W)$, leaving no spurious divergences in the $m_i \to 0$ limit.

To compute the differential decay rate in terms of the Wilson coefficients, we use the two-loop QCD corrected value of $C_7^{\text{eff}}(m_c)$ as obtained in Ref. [10], compute $C_9^{\text{eff}}(m_c)$ from Eq. (13), and $C_{10}(m_c) = C_{10}(M_W)$ from Eq. (12). The differential decay rate in the approximation of massless leptons is given by

$$\begin{aligned} \frac{d\Gamma_{c\to u\ell^+\ell^-}}{d\hat{s}} &= \tau_D \frac{G_F^2 \alpha^2 m_c^6}{768\pi^5} (1-\hat{s})^2 \left[\left(\left|C_9^{\text{eff}}(m_c)\right|^2 + |C_{10}|^2\right)(1+2\hat{s}) \right. \\ &\quad \left. +12\, C_7^{\text{eff}}(m_c)\, \text{Re}\left[C_9^{\text{eff}}(m_c)\right] + 4\left(1+\frac{2}{\hat{s}}\right)\left|C_7^{\text{eff}}(m_c)\right|^2\right] , \end{aligned} \tag{15}$$

where τ_D refers to the lifetime of either $D^\pm$ or D^0. We estimate the inclusive branching ratios for $m_c = 1.5$ GeV, $m_s = 0.15$ GeV, $m_b = 4.8$ GeV and $m_d = 0$,

$$\mathcal{B}r^{(\text{sd})}_{D^+\to X_u^+ e^+e^-} \simeq 2\times 10^{-8} , \qquad \mathcal{B}r^{(\text{sd})}_{D^0\to X_u^0 e^+e^-} \simeq 8\times 10^{-9} . \tag{16}$$

It is interesting to point out that the dominant contributions to the rates in Eq. (16) come from the leading order mixing of O_9 with the four-quark operators $O_2^{(q)}$, the second term in Eq. (13). On the one hand and as noted above, the dominance of light-quark intermediate states in the short distance contributions is a signal of the presence of large long distance effects. On the other hand, when considering the contributions of various new physics scenarios, it should be kept in mind that these must be compared to the mixing of these operators. Shifts in the matching conditions for the Wilson coefficients C_7, C_9 and C_{10}, even when large, are not enough in most extensions of the SM. These considerations will be helpful when we evaluate what type of new physics might be relevant in these decay modes.

2.1.2 The Long Distance Contributions to $D \to X_u \ell^+\ell^-$

As a first estimate of the contributions of long distance physics we will consider the process $D \to XV \to X\ell^+\ell^-$, where $V = \phi, \rho, \omega$. We have isolated contributions from this

Table 1: Examples of $D \to PV^0 \to P\ell^+\ell^-$ Mechanism.

Mode	$\mathcal{B}r^{(\text{pole})}$	$\mathcal{B}r^{(\text{expt})}$
$D^+ \to \pi^+\phi \to \pi^+e^+e^-$	$1.8 \cdot 10^{-6}$	$< 5.2 \cdot 10^{-5}$
$D^+ \to \pi^+\phi \to \pi^+\mu^+\mu^-$	$1.5 \cdot 10^{-6}$	$< 1.5 \cdot 10^{-5}$
$D_s^+ \to \pi^+\phi \to \pi^+e^+e^-$	$1.1 \cdot 10^{-5}$	$< 2.7 \cdot 10^{-4}$
$D_s^+ \to \pi^+\phi \to \pi^+\mu^+\mu^-$	$0.9 \cdot 10^{-5}$	$< 1.4 \cdot 10^{-4}$

particular mechanism by integrating $d\Gamma/dq^2$ over each peak associated with an exchanged $V^0 = \rho^0, \omega, \phi$ and $P^0 = \eta, \eta'$. The branching ratios thus obtained (we refer to each such branching ratio as $\mathcal{B}r^{(\text{pole})}$) are in the $\mathcal{O}(10^{-6})$ range. Modes experiencing the largest effects are displayed in Table 1, where we compare our theoretically derived branching ratios with existing experimental bounds [11]. Due to the small $\eta \to \ell^+\ell^-$ and $\eta' \to \ell^+\ell^-$ branching ratios, the dominant contributions arise from V^0 exchange.

This result suggests that the long distance contributions overwhelm the short distance physics and possibly any new physics present in it. However, as we will see below this is not always the case. A more thorough treatment requires looking at all the kinematically available regions in $D \to X_u\ell^+\ell^-$, not just the resonance region. In order to do this the effect of these states can be thought of as a shift in the short distance coefficient C_9^{eff} in Eq. (13), since $V \to \ell^+\ell^-$ selects a vector coupling for the leptons. This follows from Ref. [12], which incorporates the resonant contributions to $b \to q\ell^+\ell^-$ decays via a dispersion relation for $\ell + \ell^- \to$ hadrons. This procedure is manifestly gauge invariant. The new contribution can be written via the replacement [12]

$$C_9^{\text{eff}} \to C_9^{\text{eff}} + \frac{3\pi}{\alpha^2} \sum_i \kappa_i \frac{m_{V_i}\Gamma_{V_i \to \ell^+\ell^-}}{m_{V_i}^2 - s - i m_{V_i}\Gamma_{V_i}} , \tag{17}$$

where the sum is over the various relevant resonances, m_{V_i} and Γ_{V_i} are the resonance mass and width, and the factor $\kappa_i \sim \mathcal{O}(1)$ is a free parameter adjusted to fit the non-leptonic decays $D \to XV_i$ when the V_i are on shell. We obtain $\kappa_\phi \simeq 3.6$, $\kappa_\rho \simeq 0.7$ and $\kappa_\omega \simeq 3.1$. The latter result comes from assuming $\mathcal{B}r_{D^+\to\pi^+\omega} = 10^{-3}$, since a direct measurement is not available yet.

As a first example we study the $D^+ \to \pi^+e^+e^-$ decay. The main long-distance contributions come from the ϕ, ρ and ω resonances. The η and η' effects are negligibly small. The dilepton mass distribution for this decay takes the form

$$\frac{d\Gamma}{ds} = \frac{G_F^2\alpha^2}{192\pi^5}|\vec{p}_\pi|^3\,|f_+(s)|^2 \left(\left|\frac{2m_c}{m_D}C_7^{\text{eff}} + C_9^{\text{eff}}\right|^2 + |C_{10}|^2\right) , \tag{18}$$

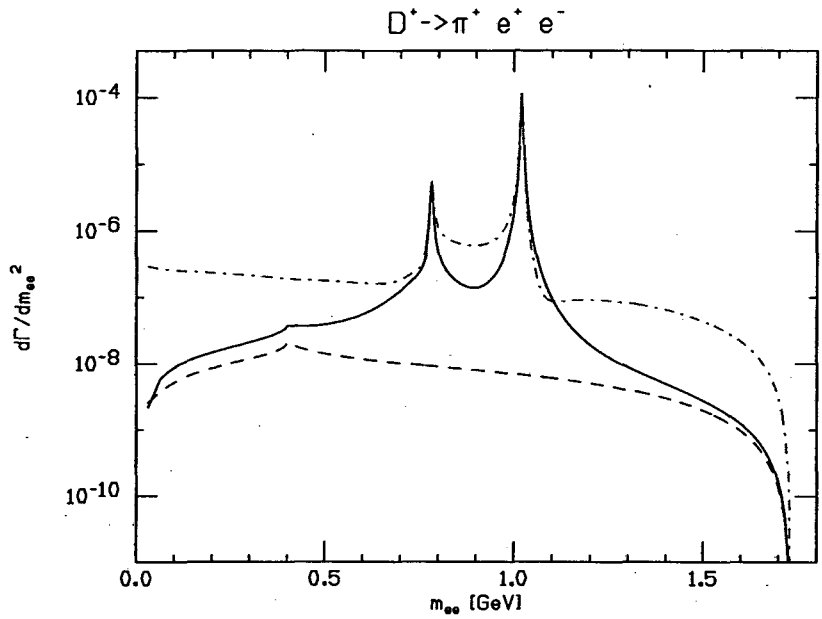

Figure 1: The dilepton mass distribution for the $D^+ \to \pi^+ e^+ e^-$, normalized to Γ_{D^+}. The solid line shows the sum of the short and the long distance SM contributions. The dashed line corresponds to the short distance contribution only. The dot-dash line includes the allowed R-parity violating contribution from Supersymmetry (see Section 3.1.2)

where $s = m_{ee}^2$ is the squared of the dilepton mass. For the form-factor $f_+(s)$ we make use of the prediction of Chiral Perturbation Theory for Heavy Hadrons [13] which at low recoil gives

$$f_+(s) = \frac{f_D}{f_\pi} \frac{g_{D^* D\pi}}{(1 - s/M_{D^*}^2)} \tag{19}$$

In Fig. 1 we plot this distribution as a function of the dilepton mass. The two narrow peaks are the ϕ and the ω, which sit on top of the broader ρ. The total rate results in $\mathcal{B}r_{D^+ \to \pi^+ e^+ e^-} \simeq 2 \times 10^{-6}$. Although most of this branching ratio comes from the intermediate $\pi^+ \phi$ state, we can see from Figure 1 that new physics effects as low as 10^{-7} can be observed as long as such sensitivity is achieved in the regions away from the ω and ϕ resonances, both at low and high dilepton mass squared.

Similarly, we can consider the decay $D^+ \to \rho^+ e^+ e^-$. Since there is less data available at the moment on the $D \to VV'$ modes, we will take the values of the κ_i in Eq. (17) from the fits to the $D^+ \to \pi^+ V$ case studied above. The total integrated branching ratio is $\mathcal{B}r_{D^0 \to \rho^0 e^+ e^-} = 2.5 \times 10^{-6}$ (*i.e.* $\mathcal{B}r_{D^+ \to \rho^+ e^+ e^-} = 4.7 \times 10^{-6}$). Again, as in the previous case, most of this rate comes from the resonance contributions but there is a region - in this case confined to the low m_{ee} region- where sensitive measurements could test the SM short distance structure of these transitions. In addition, the ρ modes contain angular information in the form of e.g. the forward-backward asymmetry for leptons.

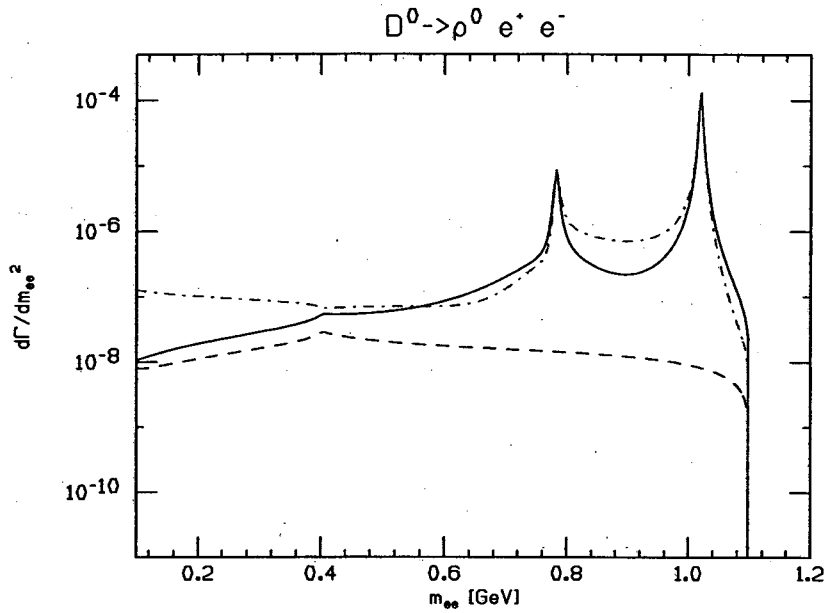

Figure 2: The dilepton mass distribution for the $D^0 \to \rho^0 e^+ e^-$, normalized to Γ_{D^0}. The solid line shows the sum of the short and the long distance SM contributions. The dashed line corresponds to the short distance contribution only. The dot-dash line includes the allowed R-parity violating contribution from Supersymmetry (see Section 3.1.2)

Since this asymmetry arises as a consequence of the interference between the vector and the axial-vector couplings of the leptons, it is negligible in the SM since vector couplings due to vector mesons overwhelm axial-vector couplings. We expand on this point and consider the possibility of large asymmetries from physics beyond the SM in Section 3.1.2. For both π and ρ modes the sensitivity to new physics effects is reserved to large $\mathcal{O}(1)$ enhancements since the long distance contributions are still important even when away from the resonances.

We finally compare our results in Figs. 1 and 2 with those obtained in Refs. [7] and [8]. In both cases we seem to numerically agree in the short distance SM prediction. However, we differ in the long distance results, which are the dominant features. For $D \to \pi \ell^+ \ell^-$ the authors of Ref. [7] make use of the factorization approximation, as well as heavy hadron chiral perturbation theory for both pseudoscalars and vector mesons. It is far from clear that the use of both this approximations in D decays is warranted. For the case of $D \to \rho \ell^+ \ell^-$, the results of Ref. [8] show a large enhancement at low q^2 when compared with Fig. 2. However, a $1/q^2$ enhancement can only appear as a result of non-factorizable contributions. This is clear from Ref.[14] and [15]: the factorization amplitude for $D \to \rho V$, when combined with a gauge invariant $(\gamma - V)$ mixing, leads to a null contribution to $D \to V \ell^+ \ell^-$. This is due to the fact that the mixing of the

operator O_2 with O_7 is non-factorizable [15]. A resonant contribution to O_7, in turn leading to a $1/q^2$ behavior, is then proportional to $C_7^{\rm eff}$ (mostly given by the O_2 mixing). In addition, when compared with the usual short distance matrix element of O_7, this resonant contribution will be further suppressed by the factor $g_V(q^2)A^{\rm nf}(q^2)$, where $g_V(q^2)$ is the $(\gamma - V)$ mixing form-factor, and $A^{\rm nf}(q^2)$ parametrizes the non-factorizable amplitude $\langle \rho V|O_7|D\rangle$, which is of $\mathcal{O}(\Lambda_{\rm QCD}/m_c)$ [16]. Thus, even if we take the on-shell values for these quantities, the resonant contribution to O_7 is likely to be below 10% of the SM short distance contribution. The actual off-shell values at low q^2 far from the resonances are likely to be even smaller. We then conclude that the $1/q^2$ enhancement is mostly given by the short distance contribution. This is only noticeable at extremely small values of the dilepton mass, so that it is likely to be beyond the experimental sensitivity in the electron modes (due to Dalitz conversion), whereas in the muon modes it lies beyond the physical region. On the other hand, the factorizable pieces contribute to the matrix elements of O_9, just as in eqn.(17), and give no enhancement at low values of q^2.

2.2 Neutrino-antineutrino Emission $D \to P\nu_\ell\bar{\nu}_\ell$

In the Standard Model, decays such as

$$D^+(p) \to \pi^+(p')\ \nu_\ell(k)\ \bar{\nu}_\ell(\bar{k}) \qquad \text{and} \qquad D^0(p) \to \bar{K}^0(p')\ \nu_\ell(k)\ \bar{\nu}_\ell(\bar{k}) \tag{20}$$

will have branching ratios which are generally (but, as we shall show, not always) too small to measure. Such decays thus represent attractive modes for new physics searches.

2.2.1 The Short Distance Contribution $c \to u\nu_\ell\bar{\nu}_\ell$

With the exception of the photon penguin, these decay modes are induced by diagrams similar to those in Fig. 1 with the charged leptons replaced with a neutrino pair. The corresponding effective hamiltonian takes the form

$$\mathcal{H}_{\rm eff} = \frac{G_F}{\sqrt{2}}\frac{\alpha}{2\pi s_W^2}\sum_{\ell=e,\mu,\tau}\left\{\lambda_s X^\ell(x_s) + \lambda_b X^\ell(x_b)\right\}(\bar{u}_L\gamma_\mu c_L)(\bar{\nu}_L^\ell\gamma^\mu\nu_L^\ell)\ . \tag{21}$$

The functions in Eq. (21) are actually given by $X^\ell(x_i) = \bar{D}(x_i, m_\ell)/2$, with the functions $\bar{D}$ given in Ref. [9]. Although we have explicitly kept the dependence on the charged lepton masses coming from the box diagrams, this is of significance only when considering the strange quark contributions with an internal tau lepton. In any case, the branching ratios in the SM are unobservably small. For instance, one has

$$\mathcal{B}r^{\rm (s.d.)}_{D^+\to X_u\nu\bar{\nu}} \simeq 1.2\times 10^{-15}\ , \qquad \mathcal{B}r^{\rm (s.d.)}_{D^0\to X_u\nu\bar{\nu}} \simeq 5.0\times 10^{-16}\ , \tag{22}$$

where the contributions of all neutrinos have been included.

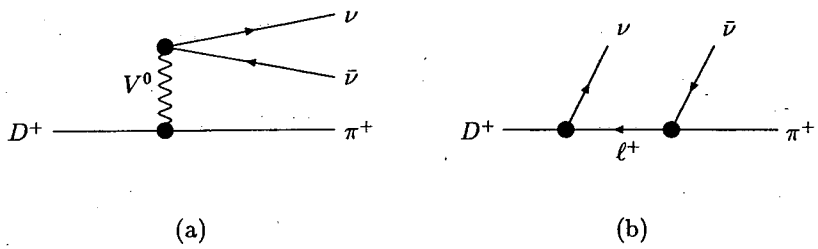

Figure 3: Some long distance contributions.

2.2.2 Long Distance Contributions to $D \to P\nu_\ell\bar{\nu}_\ell$

Long-distance contributions to the exclusive transition $D \to P\nu_\ell\bar{\nu}_\ell$ (P is a pseudoscalar meson) can have just hadrons, just leptons or both hadrons and leptons in the intermediate state. Examples of the first two cases are depicted respectively in Fig. 3(a) and Fig. 3(b).

As a simple model of the purely hadronic intermediate state, we consider in detail the nonleptonic weak process $D(p) \to \pi(p')V^0(q)$ followed by the conversion $V^0(q) \to \nu_\ell(k)\bar{\nu}_\ell(\bar{k})$, *cf* Fig. 3(a). We determine first the $V^0 \to \nu_\ell\bar{\nu}_\ell$ ($V^0 = \phi, \rho^0, \omega$) vertex, which has invariant amplitude

$$\mathcal{M}_{V^0\to\nu_\ell\bar{\nu}_\ell} \simeq \left(\frac{g_2}{2\cos\theta_w}\right)^2 \frac{1}{M_Z^2}\, \bar{u}(k)\Gamma^{\rm L}_\mu v(\bar{k})\, \langle 0|\, \sum_q J^\mu_q\, |V^0\rangle \ , \tag{23}$$

where J^μ_q is the current coupling quark q to the Z gauge boson. Only the vector part of the current contributes and we find

$$\mathcal{M}_{V^0\to\nu_\ell\bar{\nu}_\ell} \simeq \frac{2G_F}{\sqrt{2}} h_V \bar{u}(k)\epsilon^\mu_V \Gamma^{\rm L}_\mu v(\bar{k}) \ . \tag{24}$$

Using the measured electromagnetic transitions $V^0 \to \ell^+\ell^-$ ($V^0 = \rho^0, \omega, \phi$) as input, we find for the coupling h_V

$$|h_V| = \begin{cases} (3/2 - 2s_w^2)M_\phi^2/f_\phi \simeq 0.112\ \text{GeV}^2 & (V=\phi) \\ (9/8 - 2s_w^2)M_\rho^2/f_\rho - 3M_\omega^2/8f_\omega \simeq 0.107\ \text{GeV}^2 & (V=\rho) \\ -(9/8 - 2s_w^2)M_\omega^2/f_\omega + 3M_\rho^2/8f_\rho \simeq 0.008\ \text{GeV}^2 & (V=\omega) \end{cases} \ , \tag{25}$$

where we adopt the numerical values of f_ϕ, f_ρ, f_ω listed in Ref. [14].

The corresponding transition amplitude for the nonleptonic D decay process is then

$$\mathcal{M}^{(\rm V^0)}_{D\to P\nu_\ell\bar{\nu}_\ell} = G_F^2 M_D^2 \frac{1}{q^2 - (M_V - i\Gamma_V/2)^2} F(q^2) h_V(q^2)\bar{u}(k)p'\cdot\gamma\Gamma_{\rm L} v(\bar{k}) \ , \tag{26}$$

where $q \equiv p - p' = k + \bar{k}$ is the four-momentum carried by the virtual vector meson and $F(q^2)$ appears in the $D \to V^0 P$ amplitude. We find for the q^2-distribution

$$\frac{d\Gamma_{D\to P\nu_\ell\bar{\nu}_\ell}}{dq^2} = \frac{G_F^4 M_D^4}{192\pi^3}\frac{|\mathbf{p}'|}{M_D^2}\frac{F^2(q^2)h_V^2(q^2)}{(q^2 - M_V^2)^2 + \Gamma_V^2 M_V^2}\left((q\cdot p')^2 - \frac{q^2 M_V^2}{4}\right) \ . \tag{27}$$

We have used data from nonleptonic decays ($D \to P + V^0$) into pseudoscalar-vector final states to serve as input for $D^+ \to \pi^+\nu_\ell\bar{\nu}_\ell$ (ρ^0 pole), $D^0 \to \bar{K}^0\nu_\ell\bar{\nu}_\ell$ (ρ^0, ω, ϕ poles) and $D_s^+ \to \pi^+\nu_\ell\bar{\nu}_\ell$ (ω, ϕ poles). Taking the largest contributor in each category, we obtain

$$\begin{aligned} \mathcal{B}r_{D^+\to\pi^+\nu\bar{\nu}} &\simeq 5.1\times10^{-16} \qquad (V=\rho^0) \\ \mathcal{B}r_{D^0\to\bar{K}^0\nu\bar{\nu}} &\simeq 2.4\times10^{-13} \qquad (V=\phi) \\ \mathcal{B}r_{D_s^+\to\pi^+\nu\bar{\nu}} &\simeq 7.8\times10^{-15} \qquad (V=\phi)\ , \end{aligned} \tag{28}$$

where we have summed over the three neutrino flavors. Although this analysis pertains to just the amplitudes of Fig. 3(a), we believe our results reflect the order of magnitude to be expected for other hadronic intermediate states as well. All such processes lead to unmeasureably small branching ratios.

There will also be amplitudes with single lepton intermediate states, as in Fig. 3(b). For electron and muon intermediate states, the amplitude for $D(p) \to P(p')\nu_\ell(k)\bar{\nu}_\ell(\bar{k})$ is reducible to

$$\mathcal{M}^{(\text{lept.})}_{D\to P\nu_{(e,\mu)}\bar{\nu}_{(e,\mu)}} = -2G_F^2 V_{ud}V_{cd}^*\bar{u}(k)p\cdot\gamma\Gamma_{\rm L}v(\bar{k}) + \mathcal{O}(m^2_{(e,\mu)})\ . \tag{29}$$

These lead to the branching ratios

$$\mathcal{B}r_{D^+\to\pi^+\nu_{(e,\mu)}\bar{\nu}_{(e,\mu)}} \simeq 1.8\times10^{-16}\ , \qquad \mathcal{B}r_{D_s^+\to\pi^+\nu_{(e,\mu)}\bar{\nu}_{(e,\mu)}} \simeq 3.8\times10^{-15}\ , \tag{30}$$

which are again too small for detection.

There remains the case in which τ^+ propagates as the intermediate state. This differs from the above cases involving e and μ propagation in that for part of the ν_τ-$\bar{\nu}_\tau$ phase space, the intermediate τ^+ is on the mass shell. The mode $D_s^+ \to \tau^+ + \nu_\tau$ has been observed[1] with $\mathcal{B}r_{D_s^+\to\tau^++\nu_\tau} = (7\pm4)\%$ whereas $D^+ \to \tau^+ + \nu_\tau$ has not (the predicted branching ratio is $\mathcal{B}r_{D^+\to\tau^++\nu_\tau} \simeq 9.2\ 10^{-4}$). Once the on-shell τ^+ has been produced, its branching ratio to decay into a given meson can be appreciable, *e.g.* $\mathcal{B}r_{\tau\to\rho^+\bar{\nu}_\tau} \simeq 0.25$, $\mathcal{B}r_{\tau\to\pi^+\bar{\nu}_\tau} \simeq 0.11$, *etc.* Such transitions, although involving production of a $\nu\bar{\nu}$ pair in the final state, should be measurable at a B factory.

2.3 Two Photon Emission $D^0 \to \gamma\gamma$

The amplitude for the transition $D^0(p) \to \gamma(q_1,\lambda_1)\gamma(q_2,\lambda_2)$ can be expressed as

$$\mathcal{M}_{D^0\gamma\gamma} = \epsilon^\dagger_\mu(1)\epsilon^\dagger_\nu(2)\left[(q_1^\nu q_2^\mu - q_1\cdot q_2\ g^{\mu\nu})\ B_{D^0\gamma\gamma} + i\epsilon^{\mu\nu\alpha\beta}q_{1\alpha}q_{2\beta}\ C_{D^0\gamma\gamma}\right]\ . \tag{31}$$

The invariant amplitudes $B_{D^0\gamma\gamma}$ ($C_{D^0\gamma\gamma}$) are CP-conserving (CP-violating) and carry the unit of inverse energy. They contribute to the $D^0 \to \gamma\gamma$ branching ratio as

$$\mathcal{B}r_{D^0\to\gamma\gamma} = \frac{M_D^3\tau_{D^0}}{64\pi}\left[\ |B_{D^0\gamma\gamma}|^2 + |C_{D^0\gamma\gamma}|^2\ \right]\ . \tag{32}$$

[1]In this experiment, only the leptonic decay mode $\tau^+ \to \ell\nu_\ell\bar{\nu}_\tau$ was detected. [17]

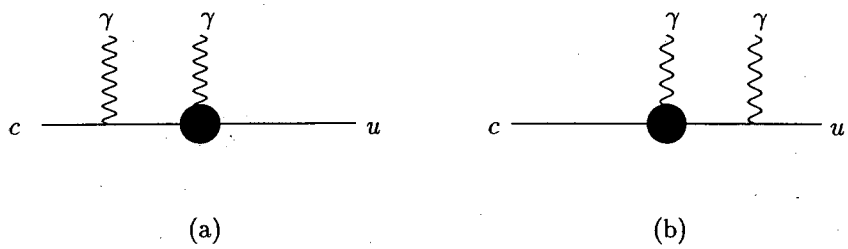

Figure 4: $1PR$ contributions to $c \to u\gamma\gamma$.

The amplitude in Eq. (31) is sometimes written in the equivalent form

$$\mathcal{M}_{D^0\gamma\gamma} = \frac{B_{D^0\gamma\gamma}}{2} F_1^{\mu\nu} B_{D^0\gamma\gamma} F_{2\mu\nu} + i\frac{C_{D^0\gamma\gamma}}{2} F_{1\mu\nu}\tilde{F}_{2\mu\nu} \quad , \tag{33}$$

where $F^{\mu\nu} \equiv i(q^\mu\epsilon^\nu - q^\nu\epsilon^\mu)$ and $\tilde{F}^{\mu\nu} \equiv \epsilon^{\mu\nu\alpha\beta}F_{\alpha\beta}/2$.

2.3.1 The Short Distance Contribution $c\bar{u} \to \gamma\gamma$

Consider the quark level transition $c \to u\gamma\gamma$. This can arise via one-particle irreducible (1PI) processes in which both photons arise from the interaction vertex or one-particle reducible (1PR) processes in which at least one of the photons is radiated from the initial state c-quark or final state u-quark.

To estimate the $c \to u\gamma\gamma$ amplitude, we make use of known results on the related process $c \to u\gamma$. According to Ref. [10], the two-loop $c \to u\gamma$ vertex is

$$\mathcal{M}^{(\text{s.d.})}_{cu\gamma} = \frac{4G_F\alpha}{\sqrt{2}\pi} A m_c \sigma_{\mu\nu}\Gamma_{\text{R}} F^{\mu\nu} \quad , \tag{34}$$

where $|A| \simeq 0.0047$. We shall use this as input to the 1PR graphs depicted in Fig. 4. The dominant contribution to the $c \to u\gamma\gamma$ amplitude involves photon emission from the u-quark. To ensure that the effect is indeed 'short-range', we follow the locality procedure employed in Ref. [18]. This yields for $c\bar{u} \to \gamma\gamma$ the amplitude

$$|\widetilde{B}^{(\text{s.d.})}_{D^0\gamma\gamma}| = |C^{(\text{s.d.})}_{D^0\gamma\gamma}| = \frac{4G_F\alpha}{3\sqrt{2}\pi}\frac{m_c}{M_D - m_c} f_D\, |A| \quad , \tag{35}$$

resulting in the branching ratio

$$\mathcal{B}r^{(\text{s.d.})}_{D^0\to\gamma\gamma} \simeq 4 \times 10^{-10} \quad , \tag{36}$$

for the choice $M_D - m_c \simeq 0.3$ GeV.

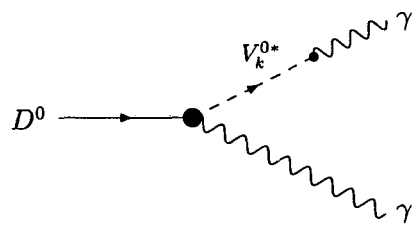

Figure 5: Vector dominance (VMD) contribution.

2.3.2 Long Distance Contributions to $D^0 \to \gamma\gamma$

We shall model long-distance contributions to the $D^0 \to \gamma\gamma$ amplitude using the vector meson dominance (VMD) mechanism and the unitarity constraint. The latter can only be done in a limited context since there will be many unitarity contributions. We will consider several one-particle intermediate states (as used in $K \to \gamma\gamma$ decays) as well as the two-particle K^+K^- intermediate state.

Vector Meson Dominance

One can view (*c.f.* Fig. 5) the $D^0 \to \gamma\gamma$ amplitude as the single VMD process

$$D^0 \to \gamma + \sum_k V_k^{0*} \to \gamma + \gamma \ . \tag{37}$$

We have previously used the VMD mechanism to model the general single-photon emission $D \to M + \gamma$ (M is some noncharm meson). [4] It is straightforward to extend our analysis to the $D^0 \to \gamma\gamma$ mode, as long as care is taken in the $D^0 \to \gamma\gamma$ amplitude to ensure gauge invariance and Bose-Einstein statistics. The amplitudes used in the $D^0(p) \to V^0(k) + \gamma(q)$ transition are defined as

$$\mathcal{M}_{DV\gamma} = \epsilon_V^{\mu\dagger}(k, \lambda_V)\epsilon_\gamma^{\nu\dagger}(q, \lambda_\gamma)\left[B_V(k_\nu q_\mu - k \cdot q g_{\mu\nu}) + iC_V \epsilon_{\mu\nu\alpha\beta} k^\alpha q^\beta\right] \ . \tag{38}$$

The VMD amplitude that we calculate is therefore of the form

$$B_{D^0\gamma\gamma}^{(\mathrm{vmd})} = \sum_i \frac{2e}{f_{V_i}} B_{V_i}\, \eta_i \ , \qquad C_{D^0\gamma\gamma}^{(\mathrm{vmd})} = \sum_i \frac{2e}{f_{V_i}} C_{V_i}\, \eta_i \ , \tag{39}$$

where f_V is the coupling for the $V^0 - \gamma$ conversion amplitude and the index 'i' refers to the specific vector meson $(\rho^0, \omega^0, \phi^0)$ and η_i is a factor accounting for the VMD extrapolation made in q^2. We take $\eta_i \simeq 1/2$ as a reasonable choice.

The values in Table 2 are somewhat lower than those which would be obtained from the $V\gamma$ amplitudes in Ref. [4]. The main reason for this is the central value for $\mathcal{B}r_{D^0 \to \phi\rho^0}$, which is a numerically significant input to the VMD calculation, cited in the Particle

Table 2: VMD Amplitudes (10^{-8} GeV^{-1}).

$D^0 \to V^0\gamma$	$B^{\rm vmd}_{D^0\gamma\gamma}$	$C^{\rm vmd}_{D^0\gamma\gamma}$
$D^0 \to \rho^0\gamma$	0.036 (1 ± 0.7)	0.045 (1 ± 0.3)
$D^0 \to \omega^0\gamma$	0.011 (1 ± 0.5)	0.012 (1 ± 0.5)
$D^0 \to \phi^0\gamma$	0.047 (1 ± 0.7)	0.036 (1 ± 0.4)

Data Group compilation has decreased by a factor of about three between 1994 and 2000. Using the central values in Table 2 and assuming positive interference between the various amplitudes to provide the maximal VMD signal gives the branching ratio

$$\mathcal{B}r^{(\rm vmd)}_{D^0\to\gamma\gamma} = \left(3.5\ {}^{+4.0}_{-2.6}\right) \cdot 10^{-8} \quad . \tag{40}$$

Single-particle Unitarity Contribution

In this category of amplitudes (*cf.* Fig. 6) the D^0 mixes with a spinless meson (either a pseudoscalar P_n or a scalar S_n) and finally decays into a photon pair,

$$\begin{aligned} B^{(\rm mix)}_{D^0\gamma\gamma} &= \sum_{P_n} \langle P_n|\mathcal{H}^{(\rm p.c.)}_{wk}|D^0\rangle \, \frac{1}{M_D^2 - M_{P_n^2}} \, B_{P_n\gamma\gamma} \\ C^{(\rm mix)}_{D^0\gamma\gamma} &= \sum_{S_n} \langle S_n|\mathcal{H}^{(\rm p.v.)}_{wk}|D^0\rangle \, \frac{1}{M_D^2 - M_{S_n^2}} \, C_{S_n\gamma\gamma} \quad . \end{aligned} \tag{41}$$

Let us consider two distinct kinds of contributions, $B^{\rm mix}_{D^0\gamma\gamma} = B^{(\rm gnd)}_{D^0\gamma\gamma} + B^{(\rm res)}_{D^0\gamma\gamma}$:

1. If the spinless meson is a ground-state particle (π^0, η or η'),[2] we have

$$B^{\rm gnd}_{D^0\gamma\gamma} = -\frac{G_F a_2 f_D \alpha}{\sqrt{2}\pi} \left[\frac{\xi_d}{\sqrt{2}} \frac{M_\pi^2}{M_D^2 - M_\pi^2} + \frac{2\xi_s - \xi_d}{3\sqrt{2}} \sum_{k=\eta,\eta'} \frac{M_k^2}{M_D^2 - M_k^2} f_k(\theta) \right] \quad , \tag{42}$$

where $a_2 \simeq -0.55$, $\theta \simeq -20^o$, $f_\eta(\theta) \equiv \cos^2\theta - 2\sqrt{2}\sin\theta\cos\theta$ and $f_{\eta'}(\theta) \equiv \sin^2\theta + 2\sqrt{2}\sin\theta\cos\theta$. The above parameterization for the two-photon vertices agrees with the values determined experimentally,

$$B_{P_n\gamma\gamma} = \begin{cases} 0.0249 \text{ GeV}^{-1} & (\pi^0) \\ 0.0275 \text{ GeV}^{-1} & (\eta) \\ 0.0334 \text{ GeV}^{-1} & (\eta') \quad . \end{cases} \tag{43}$$

[2]The kaon intermediate state is disfavored due to the small $K \to \gamma\gamma$ branching ratio.

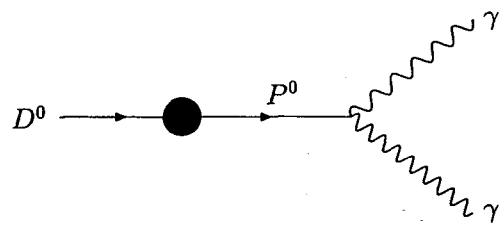

Figure 6: Weak mixing contribution.

$B^{\rm gnd}_{D^0\gamma\gamma}$ is seen to vanish, as it must, in the limit of SU(3) flavor symmetry (there $\langle\eta'|\mathcal{H}^{(\rm p.c.)}_{wk}|D^0\rangle = 0$ and the π^0, η contributions cancel). From Eq. (32), we obtain the branching ratio

$$\mathcal{B}r^{\rm gnd}_{D^0\to\gamma\gamma} \simeq 3\times 10^{-11} \quad . \tag{44}$$

2. If the intermediate meson is a spinless resonance R^0, the decay chain becomes $D^0 \to R^0 \to \gamma\gamma$. Since little is yet known about meson excitations, both the weak mixing amplitudes and the two-photon emission amplitudes must be modeled theoretically. The D^0-to-resonance weak matrix element will depend upon the flavor structure of R^0, *e.g.*

$$\langle R^0|\mathcal{H}^{(\rm p.c.)}_{wk}|D^0\rangle = -\frac{G_F a_2 f_D}{\sqrt{2}} \begin{cases} \xi_d f_R/\sqrt{2} & (R^0 = (\bar{u}u - \bar{d}d)/\sqrt{2}) \\ \xi_s f_R & (R^0 = \bar{s}s) \\ V^*_{cd}V_{us} f_R & (R^0 = \bar{s}d)) \end{cases} , \tag{45}$$

where the flavor content of R^0 is given in parentheses and estimates for resonance decay constants f_R are given in Ref. [3]. The $R^0 \to \gamma\gamma$ mode has been observed for a number of resonances and has typical branching ratios $\mathcal{B}r_{R^0\to\gamma\gamma} = \mathcal{O}(10^{-5})$ for $M_R \simeq 1 \to 1.3$ GeV, decreasing to $\mathcal{B}r_{R^0\to\gamma\gamma} = \mathcal{O}(10^{-6})$ for $M_R \geq 1.5$ GeV.

For a concrete example of the resonance mechanism, we choose $R^0 = \pi(1800)$ and assume $\mathcal{B}r_{\pi(1800)\to\gamma\gamma} \simeq 10^{-6}$. The resulting $D^0 \to \gamma\gamma$ branching ratio is

$$\mathcal{B}r^{R^0=\pi(1800)}_{D^0\to\gamma\gamma} \sim 10^{-10} \quad . \tag{46}$$

Two-particle Unitarity Contribution

In a factorization approach, the $D^0 \to K^+K^-$ amplitude is

$$\mathcal{M}_{D^0K^+K^-} = \frac{G_F M_D^2}{\sqrt{2}} V_{cs}V^*_{us} f \left[\left(1 - \frac{M_K^2}{M_D^2}\right) f_+(M_K^2) + \frac{M_K^2}{M_D^2} f_-(M_K^2)\right] \quad , \tag{47}$$

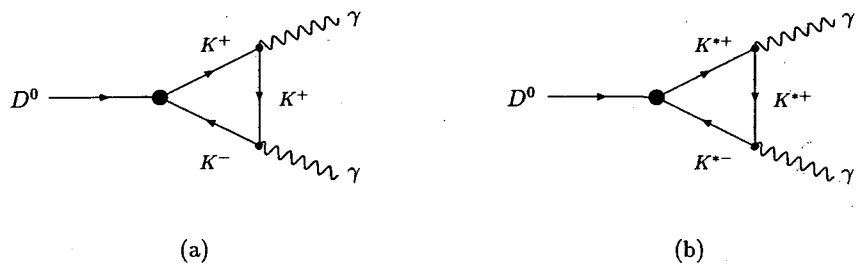

Figure 7: Unitarity contributions: (a) K^+K^-, (b) $K^{*+}K^{*-}$.

where $f_\pm$ are form factors and f is a constant containing information about QCD corrections and the kaon decay constant. A fit to the measured $D^0 \to K^+K^-$ decay rate yields

$$f\left[\left(1-\frac{M_K^2}{M_D^2}\right)f_+(M_K^2)+\frac{M_K^2}{M_D^2}f_-(M_K^2)\right]=141\ \text{MeV}\ . \tag{48}$$

The K^+K^- intermediate state contributes via unitarity to only the amplitude B of Eq. (31) and is proportional to precisely the same combination of form factors appearing in Eq. (48),

$$\mathcal{I}m\ B_{D^0\gamma\gamma}^{(K^+K^-)}=2\alpha\frac{M_K^2}{M_D^4}\sqrt{1-4M_K^2/M_D^2}\ \mathcal{M}_{D^0K^+K^-}\ , \tag{49}$$

from which we obtain

$$\mathcal{B}r_{D^0\to\gamma\gamma}^{(K^+K^-)}\sim 0.7\times 10^{-8}\ . \tag{50}$$

Summary of $D^0 \to \gamma\gamma$

Considered together, the above examples lead us to anticipate a branching ratio in the neighborhood of 10^{-8}. Our maximal (*i.e.* constructive interference) VMD signal has a central value $\mathcal{B}r_{D^0\to\gamma\gamma}^{(\text{vmd})}\simeq 3.5\cdot 10^{-8}$. The recent work of Ref. [19] provides an independent estimate of the $D^0 \to \gamma\gamma$ transition and obtains a similar order-of-magnitude result.

2.4 Lepton-antilepton Emission $D^0 \to \ell^+\ell^-$

The general form for the amplitude for the transition $D^0(p) \to \ell^+(k_+,s_+)\ell^-(k_-,s_-)$ is

$$\mathcal{M}_{D^0\to\ell^+\ell^-}=\bar{u}(k_-,s_-)\left[A_{D^0\ell^+\ell^-}\ +\ \gamma_5\ B_{D^0\ell^+\ell^-}\right]v(k_+,s_+)\ , \tag{51}$$

and the associated decay rate is

$$\Gamma_{D^0\to\ell^+\ell^-}=\frac{M_D}{8\pi}\sqrt{1-4\frac{m_\ell^2}{M_D^2}}\left[|A_{D^0\ell^+\ell^-}|^2\ +\ \left(1-4\frac{m_\ell^2}{M_D^2}\right)|B_{D^0\ell^+\ell^-}|^2\right]\ . \tag{52}$$

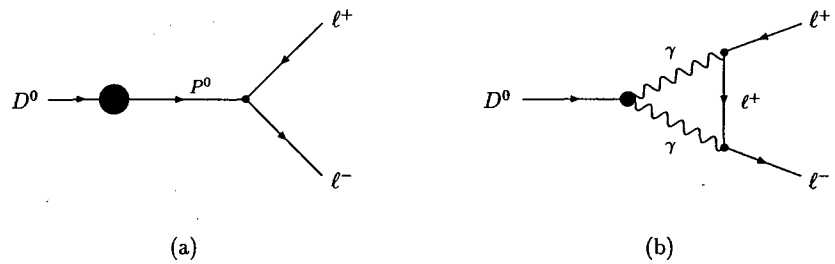

Figure 8: Unitarity contributions: (a) One-particle, (b) Two-particle $\gamma\gamma$.

2.4.1 Short Distance Contributions $c\bar{u} \to \ell^+\ell^-$

The short distance one-loop (but QCD uncorrected) transition amplitude is known to give $A^{(\text{s.d.})}_{D^0\ell^+\ell^-} \gg B^{(\text{s.d.})}_{D^0\ell^+\ell^-}$ [9], with $A^{(\text{s.d.})}_{D^0\ell^+\ell^-}$ given by

$$A^{(\text{s.d.})}_{D^0\ell^+\ell^-} \simeq \frac{G_F^2 M_W^2 f_D m_\ell}{2\pi^2} F\,, \tag{53}$$

where

$$F = \sum_{i=s,b} V_{ui}V_{ci}^* \left[\frac{3x_i^2 \ln x_i}{4(1-x_i)^2} + \frac{x_i}{1-x_i} - \frac{x_i^2}{4(1-x_i)}\right], \tag{54}$$

with $x_i = m_i^2/M_W^2$. The explicit dependence on lepton mass in the decay amplitude overwhelmingly favors the $\mu^+\mu^-$ final state over that of e^+e^- and we compute for the branching ratio,

$$\mathcal{B}r_{D^0\to\mu^+\mu^-} = \frac{G_F^4 M_W^4}{32\pi^5} f_D^2 m_\mu^2 M_{D^0}\tau_{D^0}|F|^2(1-4m_\mu^2/M_D^2)^{1/2}\,. \tag{55}$$

Upon adopting the numerical values $m_s = 0.2$ GeV, $|V_{ub}| \sim 0.004$, $|V_{cb}| \sim 0.04$, and $f_D = 0.2$ GeV, we obtain the branching fraction $\mathcal{B}r_{D^0\to\mu^+\mu^-} = 1.3 \times 10^{-19}$.

2.4.2 Long Distance Contributions to $D^0 \to \ell^+\ell^-$

In the following, we consider two long distance unitarity contributions which lead to $D^0 \to \ell^+\ell^-$ transitions. In each case, the decay amplitude is dependent on the lepton mass, and thus we shall provide numerical branching ratios only for the case $D^0 \to \mu^+\mu^-$.

Single-particle Unitarity Contribution

The single-particle 'weak-mixing' contribution to $D^0 \to \ell^+\ell^-$ can be estimated in a manner like that considered for the $D^0 \to \gamma\gamma$ transition (*cf* Eq. (41)). For definiteness, we consider the $D^0 \to \ell^+\ell^-$ parity-conserving amplitude $B_{D^0\ell^+\ell^-}$ (see Eq. (51)),

$$B^{(\text{mix})}_{D^0\ell^+\ell^-} = \sum_{P_n} \langle P_n|\mathcal{H}^{(\text{p.c.})}_{wk}|D^0\rangle \frac{1}{M_D^2 - M_{P_n^2}} B_{P_n\ell^+\ell^-}\,, \tag{56}$$

and we write $B^{(\mathrm{mix})}_{D^0\ell^+\ell^-} = B^{(\mathrm{gnd})}_{D^0\ell^+\ell^-} + B^{(\mathrm{res})}_{D^0\ell^+\ell^-}$ for the ground state (π^0, η, η') and resonance contributions.

There is little known regarding vertices governing the $P_n\mu^+\mu^-$ $(P_n = \pi^0, \eta, \eta')$ vertices. In the following, we assume these quantities have the same flavor structure as the corresponding $P_n\gamma\gamma$ vertices described earlier,[3] and obtain the the overall $P_n\mu^+\mu^-$ normalization from the measured $\eta \to \mu^+\mu^-$ mode. From this we predict for the η' (960) $\to \mu^+\mu^-$ mode a branching ratio $\mathcal{B}r_{\eta'\mu^+\mu^-} \simeq 5.6 \times 10^{-7}$, well below the current bound $\mathcal{B}r_{\eta'\mu^+\mu^-} < 10^{-4}$. The ground state contribution is then

$$\begin{aligned} B^{(\mathrm{gnd})}_{D^0\ell^+\ell^-} &= -\frac{G_F a_2 f_D B_{P\mu^+\mu^-}}{\sqrt{2}}\Bigg[\frac{\xi_d}{\sqrt{2}}\frac{M_\pi^2}{M_D^2 - M_\pi^2} \\ &+ \frac{2\xi_s - \xi_d}{3\sqrt{2}}\frac{M_\eta^2}{M_D^2 - M_\eta^2}\left(\cos^2\theta - 2\sqrt{2}\sin\theta\cos\theta\right) \\ &+ \frac{2\xi_s - \xi_d}{3\sqrt{2}}\frac{M_\eta'^2}{M_D^2 - M_\eta'^2}\left(\sin^2\theta + 2\sqrt{2}\sin\theta\cos\theta\right)\Bigg] \ , \end{aligned} \tag{57}$$

with $B_{P\mu^+\mu^-} = 3.47 \times 10^{-5}$. This leads to the branching ratio

$$\mathcal{B}r^{(\mathrm{gnd})}_{D^0\to\ell^+\ell^-} \simeq 2.5 \times 10^{-18} \ . \tag{58}$$

There can also, in principle, be intermediate state contributions from $J^P = 0^\pm$ neutral resonances $\{R^0\}$. Using the D^0-to-R^0 mixing amplitude already obtained in Eq. (45) and again identifying the resonance R^0 as $\pi(1800)$, we find

$$\mathcal{B}r^{(\pi(1800))}_{D^0\to\ell^+\ell^-} \simeq 1.8 \times 10^{-3}\frac{\Gamma_{\pi(1800)\ell^+\ell^-}}{M_{\pi(1800)}} = 1.8 \times 10^{-3}\mathcal{B}r_{\pi(1800)\to\ell^+\ell^-} \tag{59}$$

Upon assuming $\mathcal{B}r_{\pi(1800)\to\ell^+\ell^-} = 10^{-12}$ as our default branching ratio, we obtain

$$\mathcal{B}r^{(\pi(1800))}_{D^0\to\ell^+\ell^-} \simeq 5.0 \times 10^{-17}\frac{\mathcal{B}r_{\pi(1800)\to\ell^+\ell^-}}{10^{-12}} \ . \tag{60}$$

Although possibly enhanced relative to the light-meson pole contributions, the result is still tiny.

The Two-photon Unitarity Contribution

In the $K_L \to e^+e^-$ transition, the two-photon intermediate state is known to play an important role. Let us consider the contribution of this intermediate state for $D^0 \to \ell^+\ell^-$,

$$\mathcal{I}m\ \mathcal{M}_{D^0\to\ell^+\ell^-} = \frac{1}{2!}\sum_{\lambda_1,\lambda_2}\int \frac{d^3q_1}{2\omega_1(2\pi)^3}\frac{d^3q_2}{2\omega_2(2\pi)^3} \tag{61}$$

$$\times\ \mathcal{M}_{D\to\gamma\gamma}\ \mathcal{M}^*_{\gamma\gamma\to\ell^+\ell^-}(2\pi)^4\delta^{(4)}(p - q_1 - q_2) \ . \tag{62}$$

[3]This ensures that our expression will vanish in the limit of SU(3) flavor symmetry.

Upon inserting the general form of the $D^0 \to \gamma\gamma$ appearing in Eq.(33), we obtain

$$\mathcal{I}m\ A^{(\gamma\gamma)}_{D^0\ell^+\ell^-} = \alpha m_\ell B_{D^0\gamma\gamma} \ln \frac{M_D^2}{m_\ell^2} \ , \qquad \mathcal{I}m\ B^{(\gamma\gamma)}_{D^0\ell^+\ell^-} = i\alpha m_\ell C_{D^0\gamma\gamma} \ln \frac{M_D^2}{m_\ell^2} \ . \tag{63}$$

In view of the explicit dependence on lepton mass, this mechanism strongly favors the $D^0 \to \mu^+\mu^-$ transition to that of $D^0 \to e^+e^-$, and we find

$$\mathcal{B}r^{(\gamma\gamma)}_{D^0\to\mu^+\mu^-} \simeq 2.7 \times 10^{-5} \mathcal{B}r_{D^0\to\gamma\gamma} \ . \tag{64}$$

Summary of $D^0 \to \ell^+\ell^-$

The largest of our estimates, the two-photon unitarity component, for the long distance contribution to $D^0 \to \ell^+\ell^-$ favors a branching ratio somewhere in excess of 10^{-13}. More generally, it scales as 2.7×10^{-5} times the branching ratio for $D^0 \to \gamma\gamma$. With the estimate $\mathcal{B}r_{D^0\to\gamma\gamma} \geq \cdot 10^{-8}$ arrived at in the previous section, we therefore anticipate a branching ratio for $D^0 \to \ell^+\ell^-$ of at least 3×10^{-13}.

3 Potential for New Physics Contributions

3.1 Supersymmetry and Rare Charm Decays

3.1.1 Minimal Supersymmetric Standard Model

Weak scale Supersymmetry is a possible solution to the hierarchy problem. The Minimal Supersymmetric Standard Model (MSSM) is the simplest supersymmetric extension of the SM and involves a doubling of the particle spectrum by putting all SM fermions in chiral supermultiplets, as well as the SM gauge bosons in vector supermultiplets. A large number of new parameters is introduced. The soft supersymmetry breaking sector generally includes three gaugino masses, as well as trilinear scalar interactions, Higgs and sfermion masses. In general, sfermion masses are not related to fermion masses. In particular, if we choose to rotate the squark fields by the same matrices that diagonalize the quark mass matrices, squark mass matrices are not diagonal [20]. In this "super-CKM" basis, squark propagators can be expanded so that non-diagonal mass terms result in mass insertions that change the squark flavor. Thus the exchange of squarks in loops leads to FCNCs through diagrams such as the one in Fig. 9. This effect can be avoided in specific SUSY breaking scenarios such as gauge-mediation or anomaly mediation, but are present in general. This is the case, for instance if SUSY breaking is mediated by gravity. The MSSM contributions are: gluino-squark, chargino-squark and charged Higgs-quarks. This last contribution carries the same CKM structure as the SM loop diagram

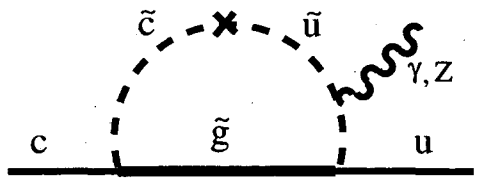

Figure 9: A typical contribution to $c \to u$ FCNC transitions in the MSSM. The cross denotes one mass insertion $(\delta^{12})_{\lambda\lambda'}$, with $\lambda, \lambda' = L, R$.

and shall be neglected for this analysis. Furthermore, the gluino-squark diagram gives the dominant contribution, so we drop the chargino diagram for the purposes of this estimate. Within the context of this Mass Insertion Approximation (MIA) and allowing for only one insertion, the contributions to the relevant Wilson coefficients from the gluino-squark diagrams are given by [21,22]

$$C_7^{\tilde{g}} = -\frac{16}{9}\frac{v^2}{M_{\rm sq}^2}\pi\alpha_s \left\{ (\delta_{12}^u)_{LL}\frac{P_{132}(u)}{4} + (\delta_{12}^u)_{LR}P_{122}(u)\frac{M_{\rm gl}}{m_c} \right\} , \tag{65}$$

for the contribution to the operator O_7 defined in Eq. (6); and

$$C_9^{\tilde{g}} = -\frac{16}{27}\frac{v^2}{M_{\rm sq}^2}\pi\alpha_s\,(\delta_{12}^u)_{LL}P_{042}(u) \ . \tag{66}$$

with the contribution to C_{10} vanishing to this order. If we allow for two mass insertions, there is a contribution to C_{10} given by

$$C_{10}^{\tilde{g}} = -\frac{1}{9}\frac{\alpha_s}{\alpha}\,(\delta_{22}^u)_{LR}(\delta_{12}^u)_{LR}P_{032}(u) \ . \tag{67}$$

In Eqs. (65), (66) and (67), $u = M_{\rm gl}^2/M_{\rm sq}^2$ and the functions $P_{ijk}(u)$ are defined as

$$P_{ijk}(u) \equiv \int_0^1 dx\ \frac{x^i(1-x)^j}{(1-x+ux)^k} \ . \tag{68}$$

In addition, the operator basis can be extended by the "wrong chirality" operators O_7', O_9' and O_{10}', obtained by switching the quark chiralities in Eqs. (6) and (7). The gluino-squark contributions to the corresponding Wilson coefficients are

$$C_7'^{\tilde{g}} = -\frac{16}{9}\frac{v^2}{M_{\rm sq}^2}\pi\alpha_s \left\{ (\delta_{12}^u)_{RR}\frac{P_{132}(u)}{4} + (\delta_{12}^u)_{LR}P_{122}(u)\frac{M_{\rm gl}}{m_c} \right\} , \tag{69}$$

$$C_9'^{\tilde{g}} = -\frac{16}{27}\frac{v^2}{M_{\rm sq}^2}\pi\alpha_s\,(\delta_{12}^u)_{RR}P_{042}(u) \ , \tag{70}$$

$$C_{10}'^{\tilde{g}} = -\frac{1}{9}\frac{\alpha_s}{\alpha}\,(\delta_{22}^u)_{LR}(\delta_{12}^u)_{LR}P_{032}(u) \ , \tag{71}$$

where the expression for $C_{10}'^{\tilde{g}}$ is also obtained with two mass insertions.

As was noted in Refs. [21,22], in both $C_7^{\tilde{g}}$ and $C_7'^{\tilde{g}}$ the term in which squark chirality labels are mixed introduces the enhancement factor $M_{\tilde{g}}/m_c$. In the SM the chirality flip needed in O_7 has to be brought about by a flip of one external quark line, bringing a factor of m_c included in the operator's definition[4]. On the other hand, in the gluino-squark diagram the insertion of $(\delta_{12}^u)_{RL}$ forces the chirality flip to take place in the gluino line, thus introducing the $M_{\tilde{g}}$ factor which replaces m_c.

The most stringent bounds that apply to the non-universal soft breaking terms $(\delta_{12}^u)_{\lambda\lambda'}$ come from the experimental searches for $D^0 - \bar{D}^0$ mixing[5]. The current CLEO bound [6] implies [22]

$$\frac{1}{2}\left\{\left(\frac{\Delta m_D}{\Gamma_{D^0}}\right)^2 \cos\delta + \left(\frac{\Delta\Gamma_D}{2\Gamma_{D^0}}\right)^2 \sin\delta\right\} < 0.04\% \ , \tag{72}$$

where δ is a strong relative phase between the Cabibbo-allowed and the doubly Cabibbo-suppressed $D^0 \to K\pi$ decays. Neglecting this phase, results in the bounds obtained in Ref. [22], which we collect in Table 3. The bounds of Table 3 were obtained assuming

$M_{\tilde{g}}^2/M_{\tilde{q}}^2$	$(\delta_{12}^u)_{LL}$	$(\delta_{12}^u)_{LR}$
0.3	0.03	0.04
1.0	0.06	0.02
4.0	0.14	0.02

Table 3: Bounds on $(\delta_{12}^u)_{LL}$, $(\delta_{12}^u)_{LR}$ from $D^0 - \bar{D}^0$ mixing [6] (neglecting the strong phase). All bounds should be multiplied by $(M_{\tilde{q}}/500$ GeV).

that $(\delta_{12}^u)_{RR} = 0$ and $(\delta_{12}^u)_{LR} = (\delta_{12}^u)_{RL}$. These assumptions have virtually no impact on the size of the effect. In order to estimate the effects in $c \to u\ell^+\ell^-$ transitions we need to specify $M_{\tilde{g}}$ and $M_{\tilde{q}}$. We consider four cases: (I): $M_{\tilde{g}} = M_{\tilde{q}} = 250$ GeV; (II): $M_{\tilde{g}} = 2\,M_{\tilde{q}} = 500$ GeV; (III): $M_{\tilde{g}} = M_{\tilde{q}} = 1000$ GeV and (IV): $M_{\tilde{g}} = (1/2)\,M_{\tilde{q}} = 250$ GeV. We first look at $D^+ \to \pi^+e^+e^-$. In Fig. 10 we plot the dilepton mass distribution *vs* the dilepton mass. Although the net effect is relatively small in the total rate ($\simeq 20\%$ or smaller), the enhancement due to the SUSY contributions is most conspicuous away from the vector resonances, particularly for low dilepton masses. Sensitivities of the order of $10^{-7} - 10^{-8}$ will be necessary to see these effects. On the other hand, the decays to a vector meson, just as $D \to \rho e^+e^-$ are even more sensitive, as it can be seen from Fig. 11. Almost the entire effect lies in the low m_{ee} region. This is due mostly to the contributions of $(\delta_{12}^u)_{RL}$ to C_7 and C_7' in Eqs. (65) and (69), enhanced by the ratio $M_{\tilde{g}}/m_c$ as discussed

[4]The m_s term is neglected.

[5]Bounds obtained from charge and color breaking (CCB) and bounding the potential from below (UFB) [23] apply to the trilinear terms but not to the squark mass terms. Thus, unless the squark mass matrices are kept diagonal, CCB and UFB arguments cannot be used to constrain the non-universal mass insertions.

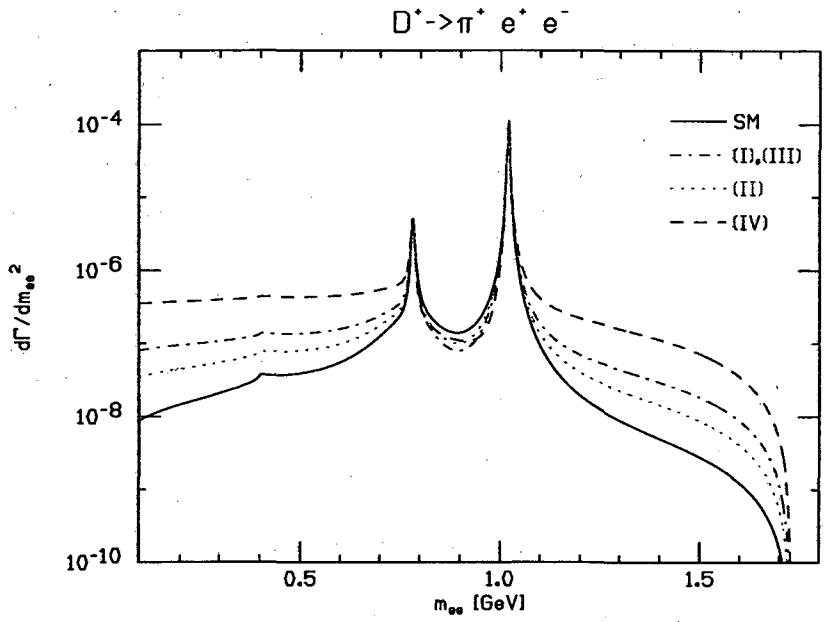

Figure 10: The dilepton mass distribution for $D^+ \to \pi^+ e^+ e^-$ (normalized to Γ_{D^+}), in the MSSM with non-universal soft breaking effects. The solid line is the SM; (I): $M_{\tilde{g}} = M_{\tilde{q}} = 250$ GeV; (II): $M_{\tilde{g}} = 2\,M_{\tilde{q}} = 500$ GeV; (III): $M_{\tilde{g}} = M_{\tilde{q}} = 1000$ GeV and (IV): $M_{\tilde{g}} = (1/2)\,M_{\tilde{q}} = 250$ GeV.

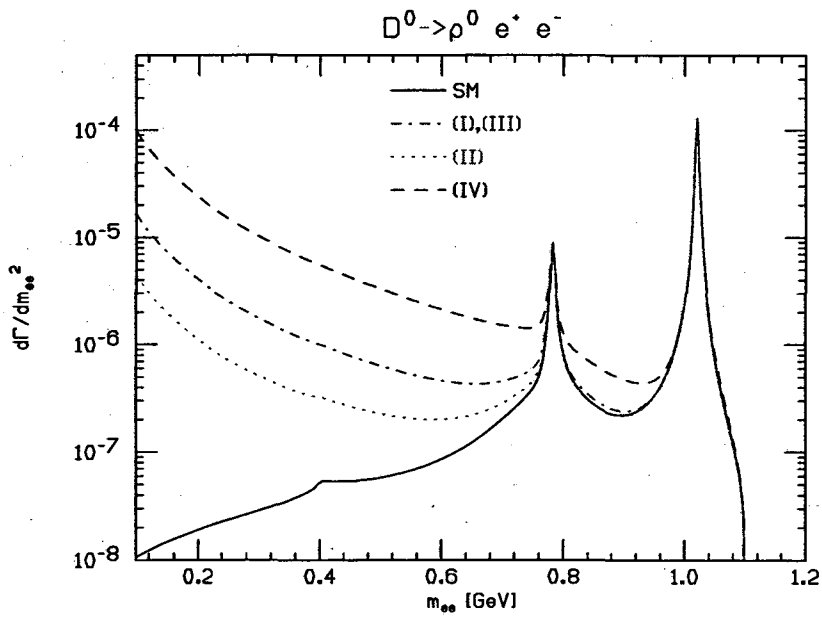

Figure 11: The dilepton mass distribution for $D^{\to}\rho^0 e^+ e^-$ (normalized to Γ_{D^0}), in the MSSM with non-universal soft breaking effects. The solid line is the SM; (I): $M_{\tilde{g}} = M_{\tilde{q}} = 250$ GeV; (II): $M_{\tilde{g}} = 2\,M_{\tilde{q}} = 500$ GeV; (III): $M_{\tilde{g}} = M_{\tilde{q}} = 1000$ GeV and (IV): $M_{\tilde{g}} = (1/2)\,M_{\tilde{q}} = 250$ GeV.

above. These terms get lifted at low $q^2 = m_{ee}^2$ due to the photon propagator (see for instance Eq. (15) for the inclusive decays). This low q^2 enhancement of the O_7 contribution is present in exclusive modes with vector mesons such as $D \to \rho\ell^+\ell^-$, but not in modes with pseudoscalars, such as $D \to \pi\ell^+\ell^-$, since gauge invariance forces a cancellation of the $1/q^2$ factor (*e.g.* see Eq. (18)). This is apparent from a comparison of the low dilepton mass region between Figs. (10) and (11). Thus, the $D \to \rho\ell^+\ell^-$ decays are considerably more sensitive to non-universal soft breaking in the MSSM. The case with the largest effect (case (IV) dashed line in Fig. (11)) gives $\mathcal{B}r_{D^0\to\rho^0 e^+e^-} \simeq 1.3 \times 10^{-5}$, about a factor of five times larger than the SM prediction given in Sect. 2.1.2. The current experimental bound on this mode is [24] $\mathcal{B}r^{\rm exp}_{D^0\to\rho^0 e^+e^-} < 1.2 \times 10^{-4}$. The somewhat more stringent bound $\mathcal{B}r^{\rm exp}_{D^0\to\rho^0\mu^+\mu^-} < 2.2 \times 10^{-5}$ should be compared to $\mathcal{B}r_{D^0\to\rho^0\mu^+\mu^-} \simeq 1.3 \times 10^{-6}$, also obtained in case (IV). Thus, data from rare charm decays with sensitivities of 10^{-6} and better will soon constrain the MSSM parameter space.

3.1.2 R Parity Violation

The assumption of R-parity conservation in the MSSM is not the only way of avoiding baryon and lepton number violating terms in the super-potential.Other symmetries can be invoked to prohibit rapid proton decay (*e.g.* baryon-parity, lepton-parity) that would allow R parity violation. The R-parity violating super-potential can be written as[6]

$$\mathcal{W}_{R_p} = \epsilon_{ab}\left\{\frac{1}{2}\lambda_{ijk}L_i^a L_j^b \bar{E}_k + \lambda'_{ijk}L^a Q_j^b \bar{D}_k + \frac{1}{2}\epsilon_{\alpha\beta\gamma}\lambda''_{ijk}\bar{U}_i^\alpha \bar{D}_j^\beta \bar{D}_k^\gamma\right\} , \tag{73}$$

where L, Q, $\bar{E}$, $\bar{U}$ and $\bar{D}$ are the chiral super-fields in the MSSM. The $SU(3)$ color indices are denoted by $\alpha, \beta, \gamma = 1, 2, 3$, the $SU(2)_L$ indices by $a, b = 1, 2$ and the generation indices are $i, j, k = 1, 2, 3$. The fields in Eq. (73) are in the weak basis. Relevant for the rare charm decays we consider here is the λ'_{ijk} term, which can give rise to tree-level contributions through the exchange of squarks to decay modes such as $D \to X\ell^+\ell^-$, $D \to \ell^+\ell^-$, as well as the lepton-flavor violating $D \to X\mu^+e^-$ and $D \to \mu^+e^-$. Before considering the FCNC effects in D decays, we need to rotate the fields to the mass basis. This leads to

$$\mathcal{W}_{R_p} = \tilde{\lambda}'_{ijk}\left[N_i V_{jl} D_l - E_i U_j\right]\bar{D}_k + \cdots \tag{74}$$

where V is the CKM matrix and we define

$$\tilde{\lambda}'_{ijk} \equiv \lambda'_{irs}\mathcal{U}^L_{rj}\mathcal{D}^{*R}_{sk} . \tag{75}$$

Here, $\mathcal{U}^L$ and $\mathcal{D}^R$ are the matrices used to rotate the left-handed up and right-handed down quark fields to the mass basis. As written in terms of component fields, this interaction

[6]We ignore bilinear terms, not relevant to our discussion of FCNC effects.

now reads

$$\mathcal{W}_{\lambda'} = \tilde{\lambda}'_{ijk}\Big\{V_{jl}[\tilde{\nu}^i_L \bar{d}^k_R d^l_L + \tilde{d}^l_L \bar{d}^k_R \nu^i_L + (\tilde{d}^k_R)^*(\bar{\nu^i_L})^c d^l_L] - \tilde{e}^i_L \bar{d}^k_R u^j_L - \tilde{u}^j_L \bar{d}^k_R e^i_L - (\tilde{d}^k_R)^*(\bar{e^i_L})^c u^j_L\Big\} \ . \tag{76}$$

The last term in Eq. (76) can give rise to the processes $c \to u\ell\ell'$ at tree level via the exchange of a down squark. This leads to effects that are proportional to $\tilde{\lambda}'_{i2k}\tilde{\lambda}'_{i1k}$ with $i = 1, 2$. Constraints on these coefficients exist already in the literature. For instance, tight bounds are obtained in Ref. [25] from $K^+ \to \pi^+\nu\bar{\nu}$ by assuming that only one R-parity violating coupling satisfies $\tilde{\lambda}'_{ijk} \neq 0$. We update this bound by using the latest experimental result [26] $\mathcal{B}r_{K^+\to\pi^+\nu\bar{\nu}} = (1.5^{+3.4}_{-1.2}) \times 10^{-10}$, which turns into $\tilde{\lambda}'_{ijk} < 0.005$. However, this bound can be avoided altogether if the assumptions are changed. For instance, if instead of only one $\tilde{\lambda}'_{ijk} \neq 0$ we have only one no-null term in the overall factor $\tilde{\lambda}'_{ijk}V_{jl}$, then there is only one term involving down quark fields and there is no possible FCNC in the down sector [25]. In this particular case, large effects are possible in the up sector for observables such as D^0-$\bar{D}^0$ mixing and rare decays. In Ref. [25] a rather loose bound on the remaining coupling is obtained from D^0 mixing. This could result in very large effects in $c \to u\ell\ell'$ decays. Here, we will take a more conservative approach and make use of more model-independent bounds. The necessary bounds for processes of interest are collected in Table 4.

$\tilde{\lambda}'_{11k}$	$\tilde{\lambda}'_{12k}$	$\tilde{\lambda}'_{21k}$	$\tilde{\lambda}'_{22k}$
$0.02^{(a)}$	$0.04^{(a)}$	$0.06^{(b)}$	$0.21^{(c)}$

Table 4: Most stringent (2σ) bounds for the R-parity violation couplings entering in rare D decays, from (a) charged current universality; (b) R_π and (c) $D \to K\ell\nu$. See Ref. [27] for details. All numbers should be multiplied by $(m_{\tilde{d}^k_R}/100$ GeV).

The bounds in Table 4 are collected most recently in Ref. [27]. The charged current universality bounds assume three generations. The π decay bound is given by the quantity $R_\pi = \Gamma_{\pi\to e\nu}/\Gamma_{\pi\to\mu\nu}$. The $D \to K\ell\nu$ bounds were first obtained in Ref. [28].

We consider first the contributions to $c \to u\ell^+\ell^-$. The tree level exchange of down squarks results, from Eq. (76), in the effective interaction

$$\delta\mathcal{H}_{\text{eff}} = -\frac{\tilde{\lambda}'_{i2k}\tilde{\lambda}'_{i1k}}{m^2_{\tilde{d}^k_R}} (\bar{\ell_L})^c c_L \ \bar{u}_L(\ell_L)^c \ , \tag{77}$$

which after Fierzing results in

$$\delta\mathcal{H}_{\text{eff}} = -\frac{\tilde{\lambda}'_{i2k}\tilde{\lambda}'_{i1k}}{2m^2_{\tilde{d}^k_R}} (\bar{u}_L\gamma_\mu c_L)(\bar{\ell}_L\gamma^\mu\ell_L) \ . \tag{78}$$

This corresponds to shifts in the Wilson coefficients C_9 and C_{10} at the high energy scale given by

$$\delta C_9 = -\delta C_{10} = \frac{s^2\theta_W}{2\alpha^2}\left(\frac{M_W}{m_{\tilde{d}_R^k}}\right)^2 \tilde{\lambda}'_{i2k}\tilde{\lambda}'_{i1k} \ . \tag{79}$$

The content of Eq. (79) translates into bounds on δC_9 and δC_{10}. Notice that they are independent of the squark mass, which cancels the one appearing in the denominator coming from the propagator.

If we now specify $\ell = e$ and use the bounds from Table 4 we get

$$\delta C_9^e = -\delta C_{10}^e = 1.10\left(\frac{\tilde{\lambda}'_{12k}}{0.04}\right)\left(\frac{\tilde{\lambda}'_{11k}}{0.02}\right) \ . \tag{80}$$

This modification of the Wilson coefficients results in the dot-dashed lines of Figs. 1 and 2 corresponding to $D^+ \to \pi^+e^+e^-$ and $D^0 \to \rho^0e^+e^-$ respectively. The effect in these rates is small, of order 10% at most, whereas the experimental bounds are a factor of 20 above this level in the best case (the pion mode).

On the other hand, for $\ell = \mu$ we obtain

$$\delta C_9^\mu = -\delta C_{10}^\mu = 17.4\left(\frac{\tilde{\lambda}'_{22k}}{0.21}\right)\left(\frac{\tilde{\lambda}'_{21k}}{0.06}\right) \ . \tag{81}$$

But these values violate the experimental bounds of Refs. [24,29] $\mathcal{B}r^{\rm exp}_{D^+\to\pi^+\mu^+\mu^-} < 1.5 \times 10^{-5}$ and $\mathcal{B}r^{\rm exp}_{D^0\to\rho^0\mu^+\mu^-} < 2.2 \times 10^{-5}$. Thus we derive the following new bound on the product of R-parity violating couplings,

$$\tilde{\lambda}'_{22k}\,\tilde{\lambda}'_{21k} < 0.004 \ , \tag{82}$$

which arises from the $D^+ \to \pi^+\mu^+\mu^-$ mode. This translates into potentially large effects in both these modes as is shown in Figs. 12 and 13.

In Figure 12 we plot the dimuon mass distribution *vs* the dimuon mass for $D^+ \to \pi^+\mu^+\mu^-$. The solid line, corresponding to the SM prediction and including both the short and long distance pieces, is clearly dominated by the latter through the presence of the vector meson resonances (see the discussion in Section 2.1.2). The dashed line includes the contribution of R parity violation given by Eq. (77), with the R-parity violating coefficients bounded by the experimental value of the branching fraction in Ref. [24]. It can be seen that *away from the resonances* there is an important window for the discovery of new phenomena, and in particular R parity violation in SUSY theories.

The situation is similar to the $D^0 \to \rho^0\mu^+\mu^-$ distribution, plotted in Figure 13. Here, the dashed line is obtained by making use of the bound in Eq. (82) coming from the $\pi^+\mu^+\mu^-$ mode as explained above. This results in an upper bound for the R parity

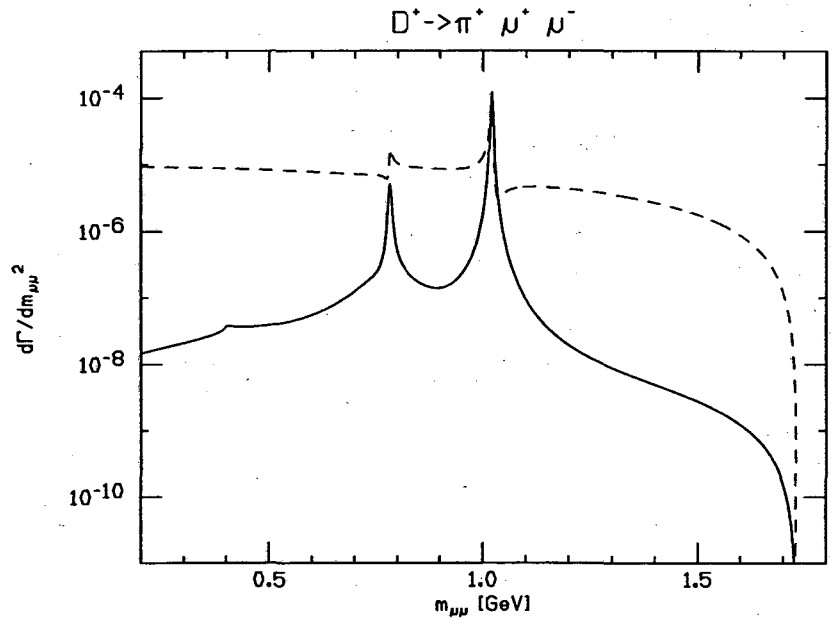

Figure 12: The dilepton mass distribution for $D^+ \to \pi^+\mu^+\mu^-$ (normalized to Γ_{D^+}),. The solid line shows the sum of the short and the long distance SM contributions. The dashed line includes the allowed R-parity violating contribution from Supersymmetry (see text for details)

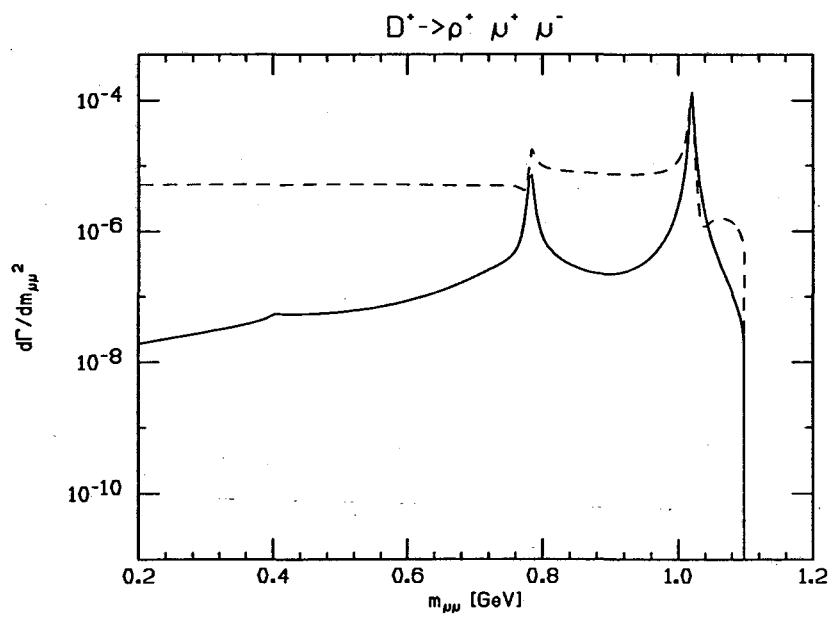

Figure 13: The dilepton mass distribution for $D^0 \to \rho^0\mu^+\mu^-$ normalized to Γ_{D^0}. The solid line shows the sum of the short and the long distance SM contributions. The dashed line includes the allowed R-parity violating contribution from Supersymmetry (see text for details.)

violating effect given by $\mathcal{B}r^{\not{R}_p}_{D^0\to\rho^0\mu^+\mu^-} < 8.7\times10^{-6}$, which is still below the experimental bound [29] $\mathcal{B}r^{\rm exp}_{D^0\to\rho^0\mu^+\mu^-} < 2.2\times10^{-5}$.

In addition to the dilepton mass distribution, this decay mode also contains angular information. For instance, we can define the forward-backward asymmetry for leptons as

$$A_{FB}(q^2) = \frac{\int_0^1 \frac{d^2\Gamma}{dxdq^2}dx - \int_{-1}^0 \frac{d^2\Gamma}{dxdq^2}dx}{\frac{d\Gamma}{dq^2}} \quad , \tag{83}$$

where $x \equiv \cos\theta$, θ is the angle between the ℓ^+ and the decaying D meson in the $\ell^+\ell^-$ rest frame. Expressions for the angular distribution $\delta\Gamma/dxdq^2$ can be found in Ref. [30] for the inclusive case and in Ref. [31] for the exclusive modes. In the SM, $A_{FB}(q^2)$ in $D^0 \to \rho^0\ell^+\ell^-$ is negligibly small. The reason for this can be seen by inspecting the numerator of the asymmetry [31]

$$A_{FB}(q^2) \sim 4\, m_D\, k\, C_{10}\left\{C_9^{\rm eff}\, g\, f + \frac{m_c}{q^2}C_7^{\rm eff}\,(f\,G - g\,F)\right\} \quad , \tag{84}$$

where k is the V three-momentum in the D rest frame, and f, g, F and G are various form-factors. Since the SM amplitude is dominated by the long distance vector intermediate states, we have $C_9^{\rm eff} \gg C_{10}$. New physics contributions that make $C_{10} \simeq C_9^{\rm eff}$ will generate a sizeable asymmetry. This is the case with R parity violating supersymmetry. For instance, taking again the values given in Eq. (82) we plot the forward-backward asymmetry for $D^0 \to \rho^0\mu^+\mu^-$ in Figure 14. In order to compute the asymmetry, we make use of $D^0 \to K^*\ell\nu$ form-factors, together with $SU(3)$ symmetry and heavy quark *spin* symmetry[7]. This gives a bound on the integrated asymmetry, $I_{FB}^{\mu\mu} \simeq 0.15$. For $D^0 \to \rho^0 e^+e^-$, we get $I_{FB}^{ee} \simeq 0.08$. Thus supersymmetry could produce very sizeable asymmetries. In general, any non-zero value of $A_{FB}(q^2)$ that is measured should be interpreted as coming from new physics.

The effective interactions of Eq. (77) also lead to a contribution to the two body decay $D^0 \to \mu^+\mu^-$. The R parity violating contribution to the branching ratio then reads

$$\mathcal{B}r^{\not{R}_p}_{D^0\to\mu^+\mu^-} = \tau_{D^0}\, f_D^2\, m_\mu^2\, m_D \sqrt{1-\frac{4m_\mu^2}{m_D^2}}\,\frac{\left(\tilde\lambda'_{22k}\tilde\lambda'_{21k}\right)^2}{64\pi\, m_{\tilde d_k}^4} \quad . \tag{85}$$

Applying the bound in Eq. (82) gives the constraint

$$\mathcal{B}r^{\not{R}_p}_{D^0\to\mu^+\mu^-} < 3.5\times10^{-6}\left(\frac{\tilde\lambda'_{12k}}{0.04}\right)^2\left(\frac{\tilde\lambda'_{11k}}{0.02}\right)^2 \quad . \tag{86}$$

The current experimental limit [24] $\mathcal{B}r_{D^0\to\mu^+\mu^-} < 5.2\times10^{-6}$ is just above this value, implying that future measurements of this decay mode will be constraining on the product of these R parity violating couplings.

[7]See the first reference cited in Ref. [31]

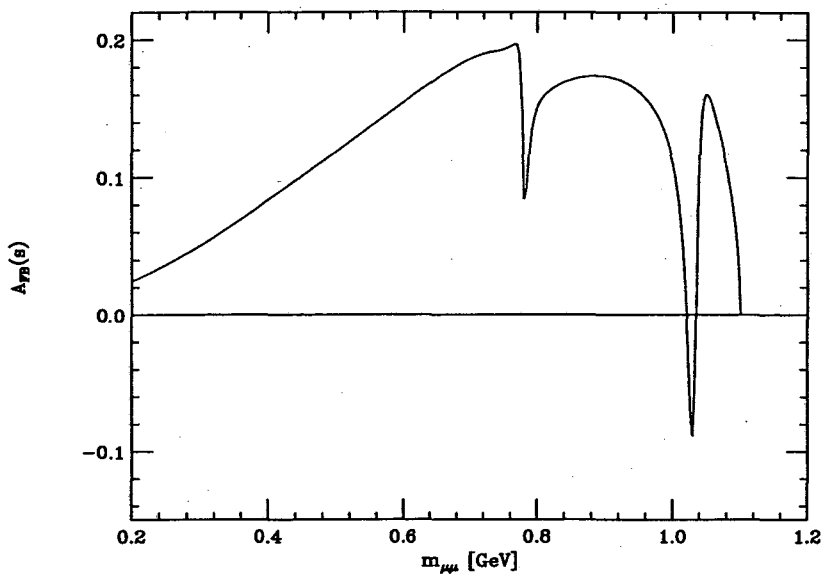

Figure 14: The lepton forward-backward asymmetry for $D^0 \to \rho^0\mu^+\mu^-$, for the bound of Eq. (82). (see text for details)

Finally, we consider the products of R parity violating couplings in Eq. (77) that lead to lepton flavor violation. The products $\tilde{\lambda}'_{11k}\tilde{\lambda}'_{22k}$ and $\tilde{\lambda}'_{21k}\tilde{\lambda}'_{12k}$ will give rise to $D^+ \to \pi^+\mu^+e^-$, for instance. This leads to

$$\delta C_9^{\mu e} = -\delta C_{10}^{\mu e} = 4.6 \times \left\{ \left(\frac{\tilde{\lambda}'_{11k}}{0.02}\right)\left(\frac{\tilde{\lambda}'_{22k}}{0.21}\right) + \left(\frac{\tilde{\lambda}'_{21k}}{0.06}\right)\left(\frac{\tilde{\lambda}'_{12k}}{0.04}\right) \right\} . \tag{87}$$

This results in $\mathcal{B}r^{\not{R}_p}_{D^+\to\pi^+\mu^+e^-} < 3 \times 10^{-5}$, to be contrasted with [24] $\mathcal{B}r^{\rm exp}_{D^+\to\pi^+\mu^+e^-} < 3.4 \times 10^{-5}$. Again here, the experiments are on the verge of being sensitive to R parity violating effects in supersymmetry. Similarly, for the corresponding two body decay we have

$$\mathcal{B}r^{\not{R}_p}_{D^0\to\mu^+e^-} < 0.5 \times 10^{-6} \times \left\{ \left(\frac{\tilde{\lambda}'_{11k}}{0.02}\right)\left(\frac{\tilde{\lambda}'_{22k}}{0.21}\right) + \left(\frac{\tilde{\lambda}'_{21k}}{0.06}\right)\left(\frac{\tilde{\lambda}'_{12k}}{0.04}\right) \right\} , \tag{88}$$

whereas the current bound is [24] $\mathcal{B}r^{\rm exp}_{D^0\to\mu^+e^-} < 8.1 \times 10^{-6}$. We summarize the results of this section in Table 5.

Finally, we point out that similar effects to those considered in this section are generated by lepto-quarks. Their exchange lead in general to effective inteactions similar to those in Eq. (77).

Decay Mode	SM	$\not{R}_p$	Exptal Limit
$D^+ \to \pi^+ e^+ e^-$	2.0×10^{-6}	2.3×10^{-6}	5.2×10^{-5}
$D^0 \to \rho^0 e^+ e^-$	4.7×10^{-6}	5.1×10^{-6}	1.0×10^{-4}
$D^+ \to \pi^+ \mu^+ \mu^-$	1.9×10^{-6}	1.5×10^{-5}	1.5×10^{-5}
$D^0 \to \rho^0 \mu^+ \mu^-$	4.5×10^{-6}	8.7×10^{-6}	2.3×10^{-4}
$D^0 \to \mu^+ \mu^-$	3.0×10^{-15}	3.5×10^{-6}	4.1×10^{-6}
$D^0 \to e^+ e^-$	few 10^{-24}	1.0×10^{-10}	6.2×10^{-6}
$D^0 \to \mu^+ e^-$	0	1.0×10^{-6}	8.1×10^{-6}
$D^+ \to \pi^+ \mu^+ e^-$	0	3.0×10^{-5}	3.4×10^{-5}
$D^0 \to \rho^0 \mu^+ e^-$	0	1.4×10^{-5}	4.9×10^{-5}

Table 5: Comparison of various decay modes between the SM and R parity violation. The third column shows how large the R parity violating effect can be. The experimental limits are from Refs. [11],[24],[29].

3.2 Extensions of Standard Model with Extra Higgses, Gauge Bosons or Fermions

In this section we summarize the results from classes of models which have additional Higgs scalar doublets, or family gauge symmetry or extra leptons. All of these give rise to Flavor Changing Couplings at tree level and potentially large rates for rare decay modes of D mesons.

3.2.1 Multiple Higgs Doublets

Many extensions of the Standard Model contain more than one Higgs scalar doublet. As is well known, this leads in general to FCNC couplings and thus to decays such as $D^0 \to \mu^+\mu^-, e^+e^-, \mu^\pm e^\mp$, *etc* at rates larger than SM expectations. In the down quark sector, there are severe constraints on such couplings from kaon decay modes. This does not necessarily lead to equally strong constraints on the up-quark sector. For example, as was shown long ago [32], it is possible that simple symmetries forbid $\Delta S = 1$ FCNC without affecting the $\Delta C = 1$ sector.

Let us write the general effective $\Delta C = 1$ interaction as

$$\beta \frac{G_F}{\sqrt{2}} \, \bar{u}\gamma_5 c \; \bar{\ell}_1 (a + b\gamma_5) \ell_2 \quad , \tag{89}$$

where β is a model dependent dimensionless number and ℓ_1, ℓ_2 refer to the pairs (μ, μ), (e, e) or (μ, e). Comparing to the mode $D^+ \to \mu^+ \nu_\mu$, one can write

$$\mathcal{B}r_{D^0 \to \ell_1 \bar{\ell}_2} \cong \frac{\beta^2}{\mid U_{cd} \mid^2} \cdot \frac{m_D^2}{m_c m_\mu} \cdot \frac{a^2 + b^2}{2} \cdot \frac{\tau_D^+}{\tau_D^0} \, \mathcal{B}r_{D^+ \to \mu^+ \nu}$$

$$\cong \; 11.35\, \beta^2 \cdot \frac{a^2+b^2}{2} \quad . \tag{90}$$

The branching ratio for the three body modes $c \to u l_i l_j$ is given by $0.343\beta^2\left(a^2+b^2\right)/2$.

We have evaluated the parameters β, a and b in several models with multiple Higgs scalar doublets and evaluated the branching ratios for rare decay modes of D^0 [32],[33]. We find that the branching ratios for these modes can be as large as:

$$\mathcal{B}r_{D^0\to\mu^+\mu^-} \sim 8.10^{-10}\,, \qquad \mathcal{B}r_{D^0\to e^+e^-} \sim 4.10^{-14}\,, \qquad \mathcal{B}r_{D^0\to\mu^\pm e^\mp} \sim 7.10^{-10}\,, \tag{91}$$

with the corresponding three body modes having branching ratios smaller than these by about a factor of 30.

3.2.2 FCNC in Horizontal Gauge Models

The Gauge sector in the Standard Model has a large global symmetry which is broken by the Higgs interaction. By enlarging the Higgs sector some subgroup of this symmetry group can be imposed on the full lagrangian to be broken spontaneously. This family symmetry can be global as well as gauged [34]. If the new gauge couplings are very weak or the gauge boson masses are very large, the difference between gauge and global symmetry is rather difficult to distinguish in practice. In general there would be FCNC effects from both gauge and scalar sectors. Here we consider the gauge contributions.

Let us construct a simple toy model as an example. Consider a family symmetry $SU(2)_H$ under which the LH quarks

$$\begin{pmatrix} u^0 \\ d^0 \end{pmatrix}_L \quad \begin{pmatrix} c^0 \\ s^0 \end{pmatrix}_L ,$$

and the corresponding LH leptons

$$\begin{pmatrix} \nu_e^0 \\ e^0 \end{pmatrix}_L \quad \begin{pmatrix} \nu_\mu^0 \\ \mu^0 \end{pmatrix}_L ,$$

transform as members of an $I_H = 1/2$ family doublet. The third family is assumed to have $I_H = 0$. In this model, the $SU(3)_H$ breaks down to $SU(2)_H \times U(1)_H$. If $\{G_\mu^i\}$ are the gauge fields generating $SU(2)_H$ and we denote $\psi_{dL}^0 = \begin{pmatrix} d^0 \\ s^0 \end{pmatrix}_L$, $\psi_{uL}^0 = \begin{pmatrix} u^0 \\ c^0 \end{pmatrix}_L$, *etc*, then the gauge interactions are:

$$g\left[\bar{\psi}_{d^0L}\,\gamma_\mu \underline{\tau}.\underline{G}^\mu \psi_d \;+ (d^0 \to u^0) \;+ (d^0 \to \ell^0)\right] \quad . \tag{92}$$

After the symmetry is broken, the mass eigenstate basis is given by

$$\begin{pmatrix} d \\ s \end{pmatrix}_L = U_d \begin{pmatrix} d^0 \\ s^0 \end{pmatrix}_L , \quad \begin{pmatrix} u \\ c \end{pmatrix}_L = U_u \begin{pmatrix} u^0 \\ c^0 \end{pmatrix}_L , \begin{pmatrix} e \\ \mu \end{pmatrix}_L = U_\ell \begin{pmatrix} e^0 \\ \mu^0 \end{pmatrix}_L \tag{93}$$

The matrices U_u, U_d and U_ℓ each need one angle and three phases. After the symmetry is broken, the three gauge bosons acquire different masses. If the phases are ignored, the matrix elements for the processes of interest are:

$$\begin{aligned}
\mathcal{M}_{D^0\to\mu^+\mu^-} &= \frac{1}{2}g^2 f_D\, m_\mu \left[\frac{\sin\ 2\theta_u \cos\theta_e}{m_3^2} - \frac{\cos\ 2\theta_u \sin 2\theta_e}{m_1^2}\right] \bar{\mu}(1+\gamma_5)\mu\ , \qquad (94)\\
\mathcal{M}_{D^0\to e^-\mu^+} &= \frac{1}{4}g^2 f_D\, m_\mu \left[\frac{\cos\ 2\theta_u \cos 2\theta_e}{m_1^2} + \frac{1}{m_2^2} + \frac{\sin 2\theta_u \sin 2\theta_e}{m_3^2}\right] \bar{\mu}(1+\gamma_5)e\ ,
\end{aligned}$$

and similar expressions for K^0 decay modes, with θ_d replacing θ_u. To proceed further, let us make the simplifying assumption that $m_1 \approx m_2 \ll m_3$ and that the mixing angles are small. Then, using the constraints from the kaon system, namely the bounds on $K_L \to e\mu$ and the known rate for $K_L \to \mu\bar{\mu}$, we find that the branching ratios for charm decay modes can be as large as:

$$\mathcal{B}r_{D^0\to\mu^+\mu^-} \sim 3.10^{-10} \qquad \text{and} \qquad \mathcal{B}r_{D^0\to\mu^\pm e^\mp} \sim 2.10^{-13}\ . \qquad (95)$$

3.2.3 Extra Fermions

Additional fermions beyond those in the three families of the SM can contribute to a variety of rare decays. Let us first consider the effect of an SU(2) singlet down-type (Q=-1/3) quark of the kind that occurs in E(6) models (an additional fourth family down-type quark belonging to a doublet would have an identical effect). This b' quark will appear in loop diagrams [35] for decays such as $D^0 \to \mu^+\mu^-$. For a mass $m_{b'} \simeq 250$ GeV, the mixing with u and c quarks $\lambda_{b'} = V_{ub'}V_{cb'}^*$ is constrained by the contribution to Δm_D. With the current bound on x_D ($x_D \equiv \Delta m_D/\Gamma_D$) of about 3% [6], $\lambda_{b'}$ has to satisfy $\lambda_{b'} < 0.003$. Then the contribution to $D^0 \to \mu^+\mu^-$ is

$$\mathcal{B}r_{D^0\to\mu^+\mu^-}(b') \approx 10^{-11}\ , \qquad (96)$$

which is two orders of magnitude above the SM value. There will be similar enhancements for modes such as $D \to \pi\ell\bar{\ell}, D \to X\ell\bar{\ell}$, *etc.*

When the SM is extended by adding extra lepton doublets or extra neutral singlets, the decay mode $D^0 \to \mu\bar{e}$ (like $K_L \to \mu\bar{e}$) can be generated only if there are non-degenerate neutrinos and nonzero neutrino mixings [36]. We display the relevant box-diagram in Fig. 15. The associated matrix element can be written as

$$\mathcal{M}_{D^0\to\mu\bar{e}} = \frac{G_F^2 M_W^2}{2\pi^2} f_D m_\mu B\ \bar{u}\Gamma_{\rm R} v\ , \qquad (97)$$

where B is given by [9]

$$B \equiv \sum_{\alpha,k} U_{\alpha\mu}^* U_{\alpha e} V_{ck}^* V_{uk} x_\alpha x_k \left[-\frac{1}{(1-x_\alpha)(1-x_k)}\right.$$

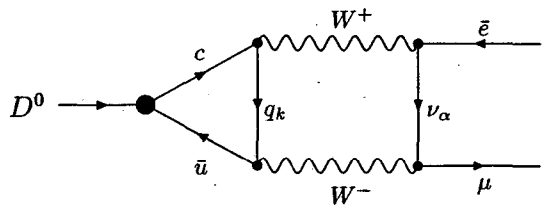

Figure 15: Box diagram in $D^0 \to \mu\bar{e}$.

$$+ \frac{1}{x_\alpha - x_k}\left(\frac{\ln x_k}{(1-x_k)^2} - \frac{\ln x_\alpha}{(1-x_\alpha)^2}\right)\Bigg] \quad . \tag{98}$$

In the above, the greek and latin indices run respectively over the neutral leptons and negatively-charged quarks, $U_{\alpha\beta}$ and V_{jk} are respectively mixing-matrix elements for leptons and quarks, and $x_k \equiv m_k^2/M_W^2$. In the excellent approximation that $x_\alpha \simeq 0$ for $\alpha = \nu_e, \nu_\mu, \nu_\tau$ and $x_i = 0$ for $i = d$, the expression for B becomes [37]

$$\begin{aligned} B &= U_{\mu N}U^*_{\alpha N}\Bigg[V^*_{cs}V_{su}\left(\frac{x_s x_N}{1-x_N} - \ln x_s + \frac{\ln x_N}{(1-x_N)^2}\right) \\ &\quad + V^*_{cb}V_{bu}\left(\frac{x_b x_N}{1-x_N} - \ln x_b + \frac{\ln x_N}{(1-x_N)^2}\right)\Bigg] \\ &\simeq 4.2\times 10^{-5}\, U^*_{Ne}U_{N\mu} \end{aligned} \tag{99}$$

for a fourth generation neutral lepton mass $m_N \simeq 50$ GeV. This varies rather slowly as m_N goes to larger values up to and beyond M_W. Then the decay rate for $D^0 \to \mu\bar{e}$ is given by

$$\Gamma_{D^0\to\mu\bar{e}} = \left[\frac{G_F^2 M_W^2 f_D m_\mu B}{4\pi^2}\right]^2 \frac{M_D}{4\pi}\left(U_{Ne}U_{N\mu}\right)^2 \quad . \tag{100}$$

The mixing $(U_{Ne}U_{N\mu})^2$ for $m_N > 50$ GeV is bounded by the limit on $\mathcal{B}r_{\mu\to e\gamma}$ to be [38,11] 5.6×10^{-8} and hence we infer

$$\Gamma_{D^0\to\mu\bar{e}} = \begin{cases} < 8.62\times 10^{-27}\ \text{GeV} \ , \\ \leq 1.3\times 10^{20}\ \text{sec}^{-1} \ . \end{cases} \tag{101}$$

The branching ratio for $D^0 \to \mu\bar{e}$ is thus bounded by

$$\mathcal{B}r_{D^0\to\mu^-e^+} \leq 5.2\times 10^{-15} \qquad \text{or} \qquad \mathcal{B}r_{D^0\to\mu^-e^+ + \mu^+e^-} \leq 1.0\times 10^{-14} \quad . \tag{102}$$

If the heavy neutral lepton N^0 is an $SU(2)$ singlet rather than a member of a doublet, the same result is obtained, even though the GIM suppression is absent [37,39]. Hence any observation of $D^0 \to \mu\bar{e}$ with $\mathcal{B}r_{D^0\to\mu\bar{e}} > 10^{-14}$ cannot be explained by mixing with a heavy neutrino.

3.3 Strong Dynamics

The possibility that new strong interactions are responsible for electroweak symmetry breaking (EWSB) and/or fermion masses has important consequences for flavor physics. The SM with one Higgs doublet already requires the presence of new dynamics at a scale Λ in order to avoid triviality bounds. The physics above the cutoff scale generates the scalar sector as bound states and has to be connected in some fashion to the the generation of flavor. For instance, technicolor theories require extended technicolor, whereas the generation of the (large) top quark mass may require a top-condensation mechanism. In general the generation of fermion mass textures leads, in one way or another, to FCNCs. Here we examine some of the potential effects in rare charm decays and their relation with other phenomenological constraints.

3.3.1 Extended Technicolor

In standard technicolor theories both fermions and techni-fermions transform under a new gauge interaction, Extended Technicolor (ETC). The condensation of techni-fermions leading to EWSB leads to fermion mass terms of the form

$$m_q \simeq \frac{g_{\rm ETC}^2}{M_{\rm ETC}^2}\langle \bar{T}T\rangle_{\rm ETC} \ . \tag{103}$$

The ETC interactions connect ordinary fermions with techni-fermions, as well as fermions and techni-fermions among themselves. The relevant sources of FCNC in technicolor models divide into two groups: those associated with the technicolor sector and those where the diagonal ETC gauge bosons acting on ordinary fermions give rise to FCNC through dimension-six operators.

The first group gives rise to operators mediated by ETC gauge bosons. These, in turn, have been shown [40] to give rise to FCNC involving the Z-boson,

$$\xi^2 \frac{m_c}{8\pi v}\frac{e}{\sin 2\theta_W} U^L_{cu} Z^\mu \ (\bar{u}_L\gamma_\mu c_L) \quad \text{and} \quad \xi^2 \frac{m_t}{8\pi v}\frac{e}{\sin 2\theta_W} U^L_{tu} U^{L*}_{tc} Z^\mu \ (\bar{u}_L\gamma_\mu c_L) \ , \tag{104}$$

where U^L is the unitary matrix rotating left-handed up-type quark fields into their mass basis and ξ is a model-dependent quantity of $\mathcal{O}(1)$. The induced flavor-conserving Z coupling was first studied in Ref. [40] and flavor-changing effects in B decays have been studied in Refs. [41,42]. The flavor-changing vertices in Eq. (104) induce contributions to $c \to u\ell^+\ell^-$. These appear mostly as a shift in the Wilson coefficient $C_{10}(M_W)$,

$$\delta C_{10} \simeq U^L_{cu}\frac{m_c}{2v}\frac{\sin^2\theta_W}{\alpha} \simeq 0.02 \ , \tag{105}$$

where we make the assumption $U^L_{cu} \simeq \lambda \simeq 0.22$ (*i.e.* one power of the Cabibbo angle) and we take $m_c = 1.4$ GeV. Although this represents a very large enhancement with respect

to the SM value of $C_{10}(M_W)$, it does not translate into a large deviation in the branching ratios. As mentioned previously, these are dominated by the mixing of the operator O_2 with O_9, leading to a very large value of $C_9^{\rm eff}$. The contribution in Eq. (105) represents only a few percent effect in the branching ratio with respect to the SM. On the other hand, the interaction in Eq. (104) can also mediate $D^0 \to \mu^+\mu^-$. The corresponding amplitude is

$$\mathcal{A}_{D^0\mu^+\mu^-} \simeq U^L_{cu} \frac{m_c}{2\pi v} \frac{G_F}{\sqrt{2}} \sin^2\theta_W f_D\, m_\mu \ , \tag{106}$$

to be compared to Eq. (53). This results in the branching ratio $\mathcal{B}r^{\rm ETC}_{D^0\to\mu^+\mu^-} \simeq 0.6\times 10^{-10}$, which although still small, is not only several orders of magnitude larger than the SM short distance contribution but also more than two orders of magnitude larger than the long distance estimates.

Finally, the FCNC vertices of the Z boson in Eq. (104) also give large contributions to $c \to u\nu\bar{\nu}$. The enhancement is considerable and results in the branching ratio

$$\mathcal{B}r^{\rm ETC}_{D^+\to X_u\nu\bar{\nu}} \simeq \xi^4 \left(\frac{U^L_{cu}}{0.2}\right)^2 2\times 10^{-9} \ . \tag{107}$$

The second group of contributions from technicolor models comes from the diagonal ETC gauge bosons. These generate four-quark interactions which refer to a mass scale constrained by D^0-$\bar{D}^0$ mixing to be approximately $M > 100$ TeV [40], thus making such effects very small in rare charm decays.

3.3.2 Top-condensation Models

Top-condensation models postulate a new gauge interaction that is strong enough to break the top-quark chiral symmetry and give rise to the large top mass. The various realizations of this basic idea have one common feature: flavor violation. Since the new interaction must be non-universal, it must mediate FCNC at tree level. This arises because the mass matrix generated between the top-condensate and whatever other flavor physics gives rise to the lighter fermion masses (*e.g.* ETC in topcolor-assisted technicolor [43]) is not aligned with the weak basis. Diagonalization of the mass matrix will then leave FCNC vertices of the so-called 'topcolor interactions' since they couple preferentially to the third generation. The exchange of top-gluons, the topcolor gauge bosons, will generate four-fermion couplings of the form

$$\begin{aligned}
&\frac{4\pi\alpha_s \cot\theta^2}{M^2} U^*_{tc}U^*_{tu}\,(\bar{u}\gamma_\mu T^a t)(\bar{t}\gamma^\mu T^a c)\\
&\frac{4\pi\alpha_s \tan\theta^2}{M^2} U_{cu}\,(\bar{u}\gamma_\mu T^a c)(\bar{c}\gamma^\mu T^a c)\\
&\frac{4\pi\alpha_s}{M^2} U_{cu}\,(\bar{u}\gamma_\mu T^a c)(\bar{\xi}\gamma^\mu T^a \xi) \ ,
\end{aligned} \tag{108}$$

where $\xi^T \equiv (t\ b)$, $U_{ij} = U^L_{ij} + U^R_{ij}$ and M is the mass of the exchanged color-octet gauge boson. The first term comes from rotating two top-quark fields and is due to a strongly coupled topgluon, reflected in the factor $\cot^2\theta \simeq 22$. The second corresponds to a topgluon which is weakly coupled to the first and second generations. In the third term, which gives the largest contribution, the topgluon couples strongly to the third generation quark current but weakly to the $(\bar{u}c)$ current, giving rise to a gluon-like coupling. The one-loop insertion of the first and/or third terms in Eq. (108) would result in contributions to the operators $\mathcal{O}_9$ and $\mathcal{O}_{10}$. However, a term analogous to the *second* term in Eq. (108) but with the $\bar{c}_L$ quark rotated to a $\bar{u}_L$ would contribute to D^0-$\bar{D}^0$ mixing. The current experimental bound on Δm_D taken from Eq. (72) implies that

$$\frac{M}{Re[U_{cu}]} > 140 \text{ TeV} . \tag{109}$$

In the standard Topcolor Assisted Techni-color models, this constraint is not binding on the top-gluon mass since the up-sector rotation matrices are taken to be nearly diagonal [44]. In any case, however it is satisfied, the bound of Eq. (109) implies that all effects in rare charm decays are negligible. Similarly, this also applies to the topcolor Z' arising from the strongly coupled $U(1)_Y$.

4 Conclusions

We have extensively evaluated the potential of rare charm decays as probes of physics beyond the SM. In Section 2 we computed the SM rates for a variety of decay modes. This complements our earlier work in Ref. [4], where we concentrated on radiative decays. We have shown that although, just as in the radiative modes, it is still true that long distance contributions dominate rates, there *are* decay modes where it is possible to access the short distance physics. This is particularly the case in $D \to X_u \ell^+\ell^-$ decay modes such as $D \to \pi\ell^+\ell^-$ and $D \to \rho\ell^+\ell^-$, where it is possible to stay away from resonance contributions in the low dilepton mass region. This can be seen in Figs. 1 and 2, where we see for low dilepton mass that the sum of long and short distance effects leaves a large window where physics beyond the SM could be seen. Although the uncertainties in our calculation of the long distance contributions to this mode are still sizeable (roughly of $\mathcal{O}(1)$) it is clear that at low dilepton masses new physics effects that are order of magnitude or more larger than the short distance SM signal can be seen. This is not the case in the resonance region where the ϕ, ω and ρ contributions take the rates to values just below current experimental bounds, in a situation analogous with radiative decays such as $D \to \rho\gamma$.

In Section 3 we explicitly explored the potential of these decays to constrain new physics. In the case of the MSSM we studied in Section 3.1.1 the sensitivity of rare

charm decays to non-universal soft breaking in the squark mass matrices. We found that large effects are possible in $D \to \pi\ell^+\ell^-$ and especially in $D \to \rho\ell^+\ell^-$, as can be seen in Figures 10 and 11. The effect in the vector mode is amplified by the heightened sensitivity of this decay channel to the photonic penguin, which carries the largest enhancement due to the fact that a gluino helicity flip replaces the usual charm quark mass insertion. We conclude that an important fraction of parameter space in the MSSM with non-universal soft breaking can be explored if sensitivities of the order of 10^{-6} to 10^{-7} in the kinematic region of interest are reached.

In Section 3.1.2 we considered the effects of R-parity violating couplings in supersymmetry. We found that the current upper limit on the decay $D \to \pi\mu^+\mu^-$ is the most constraining bound on the product $\tilde{\lambda}'_{22k}\,\tilde{\lambda}'_{21k}$ (see Eq. (82)). Thus rare charm decays already constrain R-parity violation! In Table 5 we summarized the results for the prediction of R-parity violation assuming the couplings are at their current bounds. We have also shown that the forward-backward asymmetry for leptons A_{FB} in $D^0 \to \rho^0\ell^+\ell^-$ is very sensitive to these effects (*cf* Figure 14). More generally, A_{FB} is negligibly small in the SM due to the fact that the vector coupling of leptons is enormously enhanced with respect to the axial-vector coupling by the presence of vector mesons. Thus, any observation of A_{FB} would point to new physics.

We also considered the effects of other non-supersymmetric extensions of the SM including multi-Higgs models, horizontal gauge models, a fourth generation, as well as strong dynamics such as extended technicolor and topcolor. None of these scenarios gives sizeable signals, either because the effects are intrinsically small or (as in the case of strong dynamics) because other FCNC data have already established tighter bounds on the parameter space.

We conclude that these rare charm decay modes are most sensitive to the effects of non-universal supersymmetry breaking as well as to R-parity violation couplings. It is then very important to push for increased sensitivity of the experiments, preferably to below 10^{-6} in order to highly constrain these effects. This is in stark contrast with the situation in the radiative modes, where sensitivity below $10^{-5} - 10^{-6}$ may not illuminate short distance physics. The dilepton modes should be pursued by all facilities to their highest possible sensitivity.

Acknowledgments The work of G.B was supported by the Director, Office of Science, Office of High Energy and Nuclear Physics of the U.S. Department of Energy under Contract DE-AC0376SF00098. The work of E.G. was supported in part by the National Science Foundation under Grant PHY-9801875. S.P. was suppported by the US DOE under grant DE-FG 03-94ER40833.

References

[1] J. Alcaraz *et al.*, Combined LEP and SLD Electroweak Working Groups, preprint LEPEWWG/96-02, SLD Physics Note 52.

[2] A. Datta and D. Kumbhakhar, Zeit. Phys.**C27**, 515 (1985); J. Donoghue, E. Golowich, B. Holstein and J. Trampetic, Phys. Rev., **D33**, 179 (1986); L. Wolfenstein, Phys. Lett., **B164**, 170 (1985); H. Georgi, Phys. Lett., **B297**, 353 (1992); T. Ohl *et al*, Nucl. Phys. **B403**, 605 (1993); A.A. Petrov, Phys. Rev. **D56**, 1685 (1997).

[3] E. Golowich and A.A. Petrov, Phys. Lett. **B427**, 172 (1998).

[4] G. Burdman, E. Golowich, J. Hewett and S. Pakvasa, Phys. Rev. **D52**, 6383 (1995).

[5] B. Bajc, S. Fajfer and R. J. Oakes, Phys. Rev. **D54**, 5883 (1996); S. Fajfer, S. Prelovsek and P. Singer, Eur. Phys. J. **C6**, 471 (1999).

[6] G. Brandenburg *et al.*, the CLEO collaboration, Phys. Rev. Lett. **87**, 071802 (2001).

[7] S. Fajfer, S. Prelovsek and P. Singer, Phys. Rev. **D58**, 094038 (1998).

[8] S. Fajfer, S. Prelovsek and P. Singer, "Rare charm meson decays $D \to \pi\ell^+\ell^-$ and $c \to u\ell^+\ell^-$ in SM and MSSM", hep-ph/0106333.

[9] T. Inami and C.S. Lim, Prog. Theor. Phys. **65**, 1772 (1981).

[10] C. Greub *et al*, Phys. Lett. **B382**, 415 (1996).

[11] D.E. Groom *et al.*, Eur. Phys. J. **C15**, 1 (2000).

[12] C. S. Lim, T. Morozumi and A. I. Sanda, Phys. Lett. **B218**, 343 (1989).

[13] G. Burdman and J. F. Donoghue, Phys. Lett. **B280**, 287 (1992); M. B. Wise, Phys. Rev. **D45**, 2188 (1992).

[14] E. Golowich and S. Pakvasa, Phys. Rev. **D51**, 1215 (1995).

[15] J. M. Soares, Phys. Rev. **D53**, 241 (1996).

[16] M. Beneke, G. Buchalla, M. Neubert and C. T. Sachrajda, Phys. Rev. Lett. **83**, 1914 (1999); and Nucl. Phys. **B591**, 313 (2000).

[17] M. Acciarri *et al.*, the L3 Collaboration, Phys. Lett. **B396**, 327 (1997).

[18] C-H. V. Chang, G-L. Lin and Y-P. Yao, Phys. Lett. **B415**, 395 (1997).

[19] S. Fajfer, P. Singer and J. Zupan, "The rare decay D0 $\to \gamma\gamma$", hep-ph/0104236.

[20] For a comprehensive study of FCNC effects in supersymmetry see F. Gabbiani, E. Gabrielli, A. Masiero and L. Silvestrini, Nucl. Phys. **B477**, 321 (1996). For a review see M. Misiak, S. Pokorski and J. Rosiek, in "*Heavy Flavors II*", eds. A.J. Buras and M. Lindner, Adv. Ser. Direct. High Energy Phys. **15**, 795 (1998).

[21] E. Lunghi, A. Masiero, I. Scimemi and L. Silvestrini, Nucl. Phys. **B568**, 120 (2000).

[22] S. Prelovsek and D. Wyler, Phys. Lett. **B500**, 304 (2001).

[23] J. A. Casas and S. Dimopoulos, Phys. Lett. **B387**, 107 (1996).

[24] E. Aitala *et al.*, Phys. Lett. **B462**, 401 (1999).

[25] K. Agashe and M. Graesser, Phys. Rev. **D54**, 4445 (1996).

[26] S. Adler *et al.*, E787 collaboration, Phys. Rev. Lett. **84**, 3768 (2000).

[27] B. C. Allanach, A. Dedes and H. K. Dreiner, Phys. Rev. **D60**, 075014 (1999).

[28] G. Bhattacharyya and D. Choudhury, Mod. Phys. Lett. **A10**, 1699 (1995).

[29] E. Aitala *et al.*, Phys. Rev. Lett. **86**, 3969 (2001).

[30] A. Ali, T. Mannel and T. Morozumi, Phys. Lett. **B273**, 505 (1991).

[31] G. Burdman, Phys. Rev. **D52**, 6400 (1995); Phys. Rev. **D57**, 4254 (1998).

[32] S. Pakvasa and H. Sugawara, Phys. Lett.**B73**, 61 (1978).

[33] L. Hall and S. Weinberg, Phys. Rev.**D48**, 979 (1993); A. Joshipura, Phys. Rev.**D39**, 878 (1989);K.S. Babu and S. Nandi, hep-ph/9907293; D. Atwood, L. Reina and A. Soni, Phys. Rev.**D55**, 3156 (1997); J. Bordes et al, Phys. Rev. **D60**, 013005 (1999); T. Brown et al, Phys. Lett.**B141**, 95 (1984); T.P. Cheng and M. Sher, Phys. Rev. **D35**, 3484 (1987).

[34] G. Volkov, V. A. Monich and B. Struminski, Yad. Fiz. **34**, 435 (1981); S. Weinberg, UTTG-05-91, Proceedings, High Energy Physics and Cosmology, Islamabad, M. A. B. Bég Memorial Volume; H. N. Long and V. T. Van, hep-ph/9903902. A good place for a list of references to many earlier works on horizontal gauge symmetric models is e.g.: D. S. Shaw and R. R. Volkas, Phys. Rev. **D47**, 241 (1993).

[35] K.S. Babu, X-G. He, X-Q. Li and S. Pakvasa, *Phys. Lett.* **B205**, 540 (1988).

[36] B.W. Lee, S. Pakvasa, R. Shrock and H. Sugawara, Phys. Rev. Lett. **38**, 937 (1977).

[37] P. Langacker, S. Uma Sankar and K. Schlicher, Phys. Rev. **D38**, 2841 (1988); A. Barroso *et al.*, Phys. Lett. **B134**, 123 (1984)..

[38] A. Acker and S. Pakvasa, Mod. Phys. Lett. **A7**, 1219 (1992) .

[39] Z. Gagyi-Palffy, A. Pilaftsis and K. Schilcher, Phys. Lett. B **343**, 275 (1995).

[40] R. S. Chivukula, S. B. Selipsky and E. H. Simmons, *Phys. Rev. Lett.* **69**, 575 (1992).

[41] L. J. Randall and R. Sundrum, Phys. Lett. **B312**, 148 (1993).

[42] B. Grinstein, Y. Nir and J. M. Soares, Phys. Rev. **D48**, 3960 (1993).

[43] C. T. Hill, Phys. Lett. **B266**, 419 (1991); C. T. Hill, Phys. Lett. **B345**, 483 (1995); K. Lane and E. Eichten, Phys. Lett. **B352**, 382 (1995).

[44] G. Burdman, K. D. Lane and T. Rador, Phys. Lett. **B514**, 41 (2001)

Ernest Orlando Lawrence Berkeley National Laboratory
One Cyclotron Road | Berkeley, California 94720

Prepared for the U.S. Department of Energy under Contract No. DE-AC03-76SF00098